

Coping with the Collapse: A Stock-Flow Consistent Monetary Macrodynamics of Global Warming*

Gaël Giraud[†] Florent Mc Isaac[‡] Emmanuel Bovari[§]
Ekaterina Zatsepina[¶]

July 27, 2016

Abstract

This paper presents a macroeconomic model of endogenous growth that enables us to take into consideration both the economic impact of climate change and the pivotal role of private debt. Using the Goodwin-Keen approach [25], based on the Lotka-Volterra logic, we couple its nonlinear dynamics with abatement costs. Moreover, various damage functions *à la* Nordhaus ([38]) and Dietz-Stern ([6]) reflect the loss in final production due to the temperature increase caused by the rising levels of CO₂ emissions. An empirical estimation of the model at the world-scale enables us to simulate plausible trajectories for the planetary business-as-usual scenario. Our main finding is that, even though the short-run impact of climate change on static economic fundamentals may seem *prima facie* rather minor, its long-run dynamic consequences may lead to an extreme downside. Under plausible circumstances, global warming forces the private sector to leverage in order to compensate for output losses; the private debt overhang may eventually induce a global financial collapse, even before climate change could cause serious damage to the production sector. Under more severe conditions, the interplay between global warming and debt may lead to a secular stagnation followed by a collapse in the second half of this century. We analyze the extent to which slower demographic growth or higher carbon pricing allow a global breakdown to be avoided. The paper concludes by examining the conditions under which the +1.5°C target, adopted by the Paris Agreement (2015), could be reached.

Keywords Climate change, endogenous growth, damage function, integrated assessment, collapse, stock-flow consistency, Goodwin, debt, secular stagnation.

JEL Classification Numbers: C51, D72, E12, O13, Q51, Q54

*This work benefited from the support of the Energy and Prosperity Chair. We thank Antonin Pottier and participants of the World Bank conference “The State of Economics. The State of the World” (June 16, 2016) for helpful suggestions, as well as Ivar Ekeland, Hervé Le Treut, and Nick Stern for their encouragements. All errors are, of course, our own.

[†]AFD - Agence Française de Développement, Université Paris 1 - Panthéon-Sorbonne; CES, Centre d’Economie de la Sorbonne.

[‡]AFD - Agence Française de Développement, Université Paris 1 - Panthéon-Sorbonne; CES, Centre d’Economie de la Sorbonne.

[§]AFD - Agence Française de Développement

[¶]Université Paris 1 - Panthéon-Sorbonne; CES, Centre d’Economie de la Sorbonne. This author gratefully acknowledges the financial support of ADEME.

1 Introduction

Taking advantage of over forty years of hindsight available since *The Limits to Growth* was published (Meadows *et al*(1972,1974)[34],[33], LtG in the sequel), several attempts to review how society is tracking relative to their ground-breaking modeling have addressed the question of whether the global economy is on a path of sustainability or collapse. Turner (2008, 2012, 2014)[53],[54],[55] and Hall and Day (2009)[23] (see also Jackson and Webster (2016)[24]) tend to confirm the LtG standard-run scenarios, which forecast a collapse in living standards due to resource constraints in the twenty-first century. The mechanism underlying the simulated breakdown indeed seems consistent with the increasing capital costs of peak oil and net energy (i.e., the decline of energy returned on energy invested, EROI). On the other hand, over a similar time frame, international efforts based around a series of United Nations (UN) conferences have yielded rather mixed results (Linner and Selin, 2013[29], Meadowcroft, 2013[32]). In these simulations at least, the unraveling of the global economy and environment is essentially due to the growing scarcity of natural resources (energy, minerals, water...), while climate change plays little role, if any.¹ Given the ongoing awareness of climate change damages, crystallized at the diplomatic level in the Paris Agreement of December 2015, this raises the question of whether global warming might *per se* induce a similar breakdown of the world economy.

This paper studies the conditions under which the answer to this question might be positive, assuming that the world population will follow the UN median demographic scenario (see World Population Prospects 2015 – Data Booklet[1]). At variance with the literature just mentioned, however, we explicitly model the financial side of the world economy in order to assess the possible negative feedback of private debt on the ability of the world economy to cope with planetary damages. Besides these two basic modifications – our focus on climate warming rather than resource depletion, and on explicit intertwined finance–environment dependencies – the basic mechanism at work turns out to add a new dimension, absent from the narrative initially emphasized by LtG, namely the pivotal role of private debt. Our own storyline goes as follows: losses due to environmental damages force the global productive sector to invest a growing part of its wealth in restoring and maintaining capital. As damages become more severe, current profits are no longer sufficient to fund investment. Yet, investment keeps growing, courtesy of the lending facilities provided by the world banking sector. The lingering level of debt, however, may endanger the world’s economic engine itself as it is based on the promise of future wealth creation: whenever the aggravation of climate damages prevents this promise from holding water, the productive sector may indeed become incapable of paying back its debt. Depending on the speed at which labor productivity increases compared to the severity of global warming, the shrinking of investment induced by the burden of private debt may prevent the world economy from further adapting to climate turmoil, leading ultimately to a collapse around the end of the twenty-first century.

In the same way as LtG deliberately leaves the timeline somewhat vague, the main interest of our findings lies, in our view, in the general pattern of behavior they highlight, rather than when exactly particular events might happen.

Finally, the global unraveling captured in this paper can be interpreted as the result of a debt-deflation depression in the sense given to this concept by Irving Fisher (1933)[8].

¹In LtG, of course, scenario 2 simulates a breakdown due to pollution, but the latter does not incorporate the impact of global warming.

The fact that part of the world economy might be on the verge of falling into a liquidity trap is illustrated today by the two “lost decades” of Japan, of course, but also by the recessionary state of the southern part of the Eurozone, by obstinately negative long-term interest rates on international financial markets and, last but not least, by the brutal contraction of world nominal GDP in 2015 (-6%, IMF (2016)[9]). These paradoxes may be viewed as signals that a secular decline induced by biophysical constraints is seeping the financial sphere. To the best of our knowledge, this paper offers the first narrative where debt-deflation becomes the hallmark of a possible forthcoming breakdown provoked by global warming.

1.1 The dynamics of debt

Since the financial crisis of 2007-2009, the ideas of Hyman Minsky around the intrinsic instability of a monetary market economy have experienced a significant revival. In the sequel, we adopt a mathematical formalization of Minsky’s standpoint in order to assess the role of debt dynamics in our narrative.² More precisely, our starting point is the basic Lotka-Volterra dynamics first introduced by Goodwin (1965)[15] and later extended by Keen (1995)[25]. Keen’s model (1995)[25] is a three-dimensional non-linear dynamical system describing the time evolution of the wage share, employment rate, and private debt in a closed economy. Under reasonable assumptions, this system admits, among others, two locally stable long-run equilibria: one with a finite level of debt and nonzero wages and employment rate, and another characterized by infinite debt and vanishing wages and employment (Grasselli and Costa-Lima (2012)[18]). We show how the addition of a climate backloop, modeled through appropriately selected damage and abatement functions, drives the state of the economy towards long-run equilibrium with unlimited debt, leading to a planetary downside.

Over the past thirty years many integrated assessment models (IAMs in the sequel) have been developed in order to estimate the impact of economic development on the environment. A solid body of literature compares IAM models describing their advantages and disadvantages (Schwanitz (2013)[44]). The models considered in this literature fall into one of four categories, based on the macroeconomic models they rely on: (1) welfare maximization; (2) general equilibrium; (3) partial equilibrium; and (4) cost minimization (Stanton *et al.* (2009)[47]). By contrast, our modeling approach is based on a minimal (bounded) rationality requirement on the behavior of imperfectly competitive firms, allows for multiple long-run equilibria, is stock-flow consistent (Godley and Lavoie (2012)[14]), and exhibits endogenous monetary cycles and growth, viscous prices, private debt, and underemployment. Moreover, money is endogenously created by the banking sector (Giraud and Grasselli (2016)[11]) and turns out to be non-neutral (Giraud and Kockerols (2016)[12]). The non-trivial properties of money enables the emergence of a phenomenon such as debt-deflation (Grasselli *et al.* (2015)[20]). Here, at variance with general equilibrium approaches (see, e.g., Giraud and Pottier (2015)[13]), debt-deflation need not just appear as a “black swan” – or, more precisely, a “rare” event relegated to the tail of risk distribution. On the contrary, depending on the basin of attraction where the state of the economy is driven by climate damages, the ultimate breakdown may occur as the inescapable consequence of the business-as-usual (BAU) trajectory.

²Dos Santos (2005)[43] provides a survey up to 2005 of the literature on the modeling of Minskian instability; more recent contributions include Ryoo (2010)[42] and Chiarella and Guilmi (2011)[4].

Approaches based on exogenous technology lead to three different types of answers to (some of) these questions depending on their assumptions. Somewhat oversimplifying existing approaches and assigning colorful labels, we can summarize these as follows. Nordhaus' answer is that limited and gradual interventions are necessary (see Nordhaus (2007)[38]). Optimal regulation should reduce long-run growth by only a modest amount. Stern's answer (see Stern (2013)[48]) is less optimistic. It calls for more extensive and immediate interventions, and argues that these interventions need to be in place permanently even though they may entail significant economic cost. The more pessimistic Greenpeace answer is that essentially all growth needs to come to an end in order to save the planet.

The answer provided by the thought experiments run in this paper clearly stands on the side of Stern's viewpoint: as we shall show in companion papers, fundamental bifurcations led by strong interventions may prevent the economic world from a disaster but they are not detailed here. Rather, we focus on the business-as-usual perspective, and show that gradual and marginal interventions will not suffice: too narrow an answer to the climate challenge may lead to an end of growth by disaster (not by design) and to forced degrowth.

1.2 The climate and economy interaction

By contrast with the literature based on the Ramsey-Cass-Koopmans model, we incorporate endogenous drivers of growth and allow climate change to damage these drivers. As argued indeed by Stern (Stern (2006)[49]), climate change could have long-lasting impacts on growth. We borrow from the emerging body of empirical evidence pointing in this direction (e.g., Dell *et al.* (2012)[5]), even though climatic conditions in the recent past have been relatively stable compared with what we now have to contemplate in the near future – which suggests that the “real story” might be even worse than what we are able to forecast.

Second, we consider various types of convexity of the damage function linking the increase in global mean temperature with the instantaneous reduction in output. That it might be highly convex at some temperature is strongly suggested by the literature on tipping points (see Dietz-Stern (2015)[6] and Weitzman (2012)[58]). By contrast, most existing IAM studies assume very modest curvature of the damage function. The DICE default, for instance, is quadratic, and our simulations confirm that it leads to unrealistic narratives (see Section 4.1 below).

Third, following Dietz-Stern (2015)[6] and Weitzman (2012)[58], we allow for explicit and large climate risks by considering the possibility of high values of the climate-sensitivity parameter (i.e., the increase in global mean temperature, in equilibrium, accompanying a doubling in the atmospheric concentration of CO₂). We conduct sensitivity analysis on high values, but also specify a probability distribution reflecting the latest scientific knowledge on the climate sensitivity as set out in the recent IPCC report (IPCC, 2013[51]). Its key characteristic is a fat tail of very high temperature outcomes that are assigned low probabilities. By contrast, most IAM studies have ignored this key aspect of climate risk by proceeding with a single, best-guess value for the climate sensitivity, typically corresponding to the mode of the IPCC distribution. Even though the Intentional Nationally Determined Contributions reported by the Parties to the Paris Agreement (see also IPCC, 2013[51]) should induce an average increase in temperature of 3.5°C by the end of this century, it is known that they are compatible with a 10% probability of

reaching $+6^{\circ}\text{C}$. We show that the path leading to such a level of warming would lead to a planetary collapse in the second half of this century. As written by Dietz-Stern (2015)[6]: “this is not just a ‘tail’ issue.”

The brief overview of collapses provided, e.g., in (Motesharrei *et al.*(2014)[35], p.91) not only shows the ubiquity of cycles of rise-and-collapse, but also the extent to which advanced, complex, and powerful societies are susceptible to collapse, even precipitously: “The fall of the Roman Empire, and the equally (if not more) advanced Han, Mauryan, and Gupta Empires, as well as so many advanced Mesopotamian Empires, are all testimony to the fact that advanced, sophisticated, complex, and creative civilizations can be both fragile and impermanent.” In the thought experiment suggested in Motesharrei *et al.*(2014)[35], the authors argue that the Lotka-Volterra dynamics might be the secret dynamical invariant explaining this seemingly universal process of overshoot and collapse. Here, we partially confirm this suggestion by showing that the prey-predatory dynamics, when properly introduced into a macroeconomic framework through the interplay between debt, employment, and wages, leads to a similar conclusion: the world economy, as we know it today, is not immune to such a fate.

The paper is organized as follows: Section 2 sets the scene by introducing the stock-flow consistent macroeconomic model in presence of damage and abatement costs. In Section 3, the climate module is presented, describing the interconnection between the output level, emissions, CO_2 concentration, average atmosphere temperature increase, and damages induced by climate change. Section 4 discusses the different scenarios arising from the interplay of our various key parameters. The final section summarizes the conclusions and outlines areas for future research.

2 Monetary macrodynamics

Our underlying macroeconomic model closely follows the contribution of Grasselli and Costa-Lima (2012)[18] and the literature centered around Keen’s (1995)[25] approach such as Graselli *et al.* (2012, 2014, 2015)[18],[17],[20] and Nguyen-Huu *et al.* (2014)[36] among others. This framework, based on a Lotka-Volterra logic, is motivated by the aftermath of the 2008 sub-prime mortgage crisis, during which private debt played a pivotal role in endangering the world’s macroeconomic stability. One appeal of this literature lies in its ability to formalize economic collapse as a consequence of overindebtedness. We depart from this literature, however, by endogenizing labor productivity growth, and add to the resulting structure climate-change feedback including temperature, abatement costs, and a damage function.

2.1 The basics

Absent any damages due to climate change, the “gross” real output, Y^* , is linked to the stock of productive capital, K , by a linear relationship, where, for simplicity, the capital-to-output ratio, $\nu > 0$, is assumed to be constant,

$$Y^* := \frac{K}{\nu}.$$

In this paper, $\nu \simeq 2.89$.³ Introducing a damage function as in Nordhaus (2013)[40], current production is cut so that the global supply diminishes by the quantity $\mathbf{D}\frac{K}{\nu}$, induced by global warming. Real output, Y , becomes

$$Y := (1 - \mathbf{D})\frac{K}{\nu}. \quad (1)$$

The damage function, \mathbf{D} , is an increasing nonlinear function of the global atmospheric temperature deviance relative to its value, T , in 1900, defined shortly.

Let D denote the nominal private debt of firms. Its evolution depends upon the gap between nominal investment, pI , plus nominal dividends paid to the firms' shareholders, Di , and current nominal profit, Π , that is,

$$\dot{D} := pI + Di - \Pi, \quad (2)$$

where p is the current price of consumption. The current nominal profit, Π , is

$$\Pi := pY - W - rD,$$

with W being the nominal wage bill, and r the (constant) short-term nominal interest rate.⁴ Denoting the total workforce by N , and the number of employed workers by L , the productivity of labor, the employment rate, and the nominal wage per capita are given respectively by

$$a := \frac{Y^*}{L}, \quad \lambda := \frac{L}{N} \quad \text{and,} \quad w = \frac{W}{L}. \quad (3)$$

Denoting $\omega := wL/pY$ the wage share, and $d := D/pY$ the private debt ratio, net profit becomes $\Pi = (1 - \omega - rd)pY$. In the sequel, we denote by

$$\pi := 1 - \omega - rd \quad (4)$$

the net profit share. Capital accumulation obeys the standard equation, expressed in real terms as

$$\dot{K} := I - \delta K,$$

where δ is the constant depreciation rate of capital. Net investments are equal to gross investments minus abatement costs (defined shortly) paid by investors, that is,

$$I := Y(\kappa(\pi) - \mu G), \quad (5)$$

where $\kappa(\cdot)$ is an increasing function of π , $G \in [0, 1]$ denotes the real abatement costs imposed on the economy, and $\mu \in [0, 1]$ is measuring the fraction of abatement costs paid by investors. The function $\kappa(\cdot)$ will be empirically estimated.⁵

³See Appendix E.1 for details. The extension to an endogenous capital-to-output ratio is left for further research.

⁴Here, for simplicity, r is kept constant. We shall endogenize it and analyze in depth the impact of Taylor rules in a subsequent paper.

⁵See Appendix E.4 for details. We refrain from trying to provide micro-foundations to either $\kappa(\cdot)$ or $\Phi(\cdot)$. Indeed, as shown by Mas-Colell (1995)[31], full-blown rational corporates, when they are sufficiently numerous, are exposed to an "everything-is-possible" theorem *à la* Sonnenschein-Mantel-Debreu at the aggregate level. Our phenomenological approach allows for this kind of emergence phenomena.

Here, as in both the Goodwin and Keen models, the behavior of households is fully accommodated in the sense that, given the investment function, consumption is determined by the accounting identity

$$C := Y - I = (1 - \kappa(\pi) - \mu G)Y,$$

precluding more general specification of households saving propensity.⁶ Table 1 makes explicit the stock-flow consistency of our model.

	Households	Firms	Banks	Sum
Balance Sheet				
Capital stock		pK		pK
Loan		$-D$	D	
Sum (net worth)		X^f	X^b	X
Transactions				
		current	capital	
Consumption	$-pC$	pC		
Investment		pI	$-pI$	
Accounting memo [GDP]		$[pY(1 - \mathbf{D})]$		
Wages	W	$-W$		
Interests on debt		$-rD$	rD	
Firms' net profit		$-\Pi$	Π	
Dividends	D_i		$-D_i$	
Financial Balances			$-D$	Π^b
Flow of funds				
Gross Fixed Capital Formation		pI		pI
Change in loans		$-\dot{D}$	\dot{D}	
Column sum		$\Pi - D_i$	\dot{D}	pI
Change in net worth		$\dot{X}^f = \Pi - D_i + (\dot{p} - \delta p)K$	$\dot{X}^b = \Pi^b$	\dot{X}

Table 1: Balance sheet, transactions, and flow of funds in the world economy.

It can be readily checked that, in this set-up, the accounting identity “investment = saving” always holds. This model departs from Grasselli *et al.* (2015)[20] in four ways. First, it includes damages induced by climate change. Second, we make explicit the dividends paid by firms to households. Third, as we shall see *infra*, labor productivity growth will be endogenous. Fourth, the labor force is no longer assumed to grow exponentially but rather according to a sigmoid inferred from the 15–64 age group in the United Nations scenario, World Population Prospects 2015 – Data Booklet.[1]

$$\frac{\dot{N}}{N} := q\left(1 - \frac{N}{M}\right),$$

where $M \approx 7.056$ billion is the upper bound of the labor force on Earth and q is the speed of convergence towards M (i.e., basically, the pace at which the demographic transition is assumed to take place in sub-Saharan Africa).⁷

⁶Studying the consequences of dropping Say’s law will be the task of a forthcoming paper.

⁷The estimation of the vector (q, M) is detailed in Appendix C.

2.2 Endogenous monetary cycles

The link between the real and nominal spheres of the economy is provided by a short-run wage-price dynamics taken from Grasselli and Nguyen-Huu (2014)[21].⁸

$$\frac{\dot{w}}{w} := \phi(\lambda) + \gamma i, \quad (6)$$

where $0 \leq \gamma \leq 1$, $\eta_p > 0$, $m \geq 1$, and

$$i = \frac{\dot{p}}{p} := -\eta_p \left(1 - m \frac{w}{(1 - \mathbf{D})pa} \right) + c = \eta_p(m\omega - 1) + c. \quad (7)$$

Equation (6) states that workers bargain for wages based on the current state of (un)employment (as in Keen (1995)[25]), but also take into account the observed inflation rate, i . The constant γ measures the degree of monetary illusion, with $\gamma = 1$ corresponding to the case where workers fully incorporate inflation into their bargaining (no “money illusion”). Equation (7) captures the dynamics of inflation, where the long-run equilibrium price is given by a markup, $m \geq 1$, times the unit labor cost, $W/pY = w/pa$. Observed prices converge to this long-run target through a lagged adjustment of exponential form with a relaxation time $1/\eta_p$.⁹ Whenever the consumption goods market is imperfectly competitive, $m > 1$.

The real growth rate, g , of the economy can be expressed as a function of the growth rate of capital:

$$g := \frac{\dot{Y}}{Y} = \frac{\dot{K}}{K} - \frac{\dot{\mathbf{D}}}{1 - \mathbf{D}}. \quad (8)$$

On the other hand, since $Y = (1 - \mathbf{D})aL$, it follows that

$$g = \frac{\dot{a}}{a} + \frac{\dot{L}}{L} - \frac{\dot{\mathbf{D}}}{(1 - \mathbf{D})} \quad (9)$$

Equations (8) and (9) illustrate the impact of climate change on real growth. By means of illustration, whenever labor productivity grows exogenously at rate $\dot{a}/a = \alpha > 0$, the wage share, $\omega = wL/p(1 - \mathbf{D})aL$ evolves according to

$$\frac{\dot{\omega}}{\omega} = \frac{\dot{w}}{w} - \frac{\dot{a}}{a} + \frac{\dot{\mathbf{D}}}{1 - \mathbf{D}} - i \quad (10)$$

$$= \phi(\lambda) - \alpha + \frac{\dot{\mathbf{D}}}{1 - \mathbf{D}} - (1 - \gamma)i. \quad (11)$$

Changes in the employment rate are given by

$$\begin{aligned} \frac{\dot{\lambda}}{\lambda} &= \frac{\dot{L}}{L} - \frac{\dot{N}}{N} = \frac{\dot{Y}}{Y} - \frac{\dot{a}}{a} - \frac{\dot{N}}{N} + \frac{\dot{\mathbf{D}}}{(1 - \mathbf{D})} \\ &= g - \alpha - q \left(1 - \frac{N}{M} \right) + \frac{\dot{\mathbf{D}}}{(1 - \mathbf{D})}. \end{aligned}$$

⁸See also Mankiw (2010)[30] for a justification of the short-run Philips curve.

⁹The estimation of these parameters is available in Appendix E.7. It plays a role analogous to the Calvo parameter in the neo-Keynesian literature, capturing the viscosity of prices.

It is worth mentioning that, in the short run, a more severe damage process will favor the growth of the wage share and employment rate via compensation. As we shall see, however, this positive impact is limited since, above a certain threshold, global warming induces an unraveling that may lead in the long-run to full unemployment and a zero wage share.

Absent climate damages (i.e., whenever $\mathbf{D} = 0$), equations (1) and (3) can be viewed as arising from a Leontief production function

$$Y^* = \min \left\{ \frac{K}{\nu}, aL \right\},$$

together with a minimal rationality requirement: $\frac{K}{\nu} = aL$ along any trajectory, which says that the productive sector does not hire more employees than needed, given the level of gross real output permitted by installed capital.

Finally, the prey-predatory forces underlying our dynamics are best viewed in the simple case of exponential technological progress without climate change feedback, summarized by a four-dimensional, non-linear dynamical system, where $\text{div} := D_i/pY$ is the constant share of dividend per nominal GDP distributed to households by the non-financial private sector:¹⁰

$$\begin{cases} \dot{\omega} &= \omega [\phi(\lambda) - \alpha - (1 - \gamma)i] \\ \dot{\lambda} &= \lambda \left[\frac{\kappa(\pi)}{\nu} - \delta - \alpha - \frac{\dot{N}}{N} \right] \\ \dot{d} &= d \left[r - \frac{\kappa(\pi)}{\nu} + \delta - i \right] + \kappa(\pi) - (1 - \omega) + \text{div} \\ \dot{N} &= qN \left(1 - \frac{N}{M} \right), \end{cases}$$

which is easily shown to embed a Kolmogorov type of predator-prey model (i.e., a generalized autonomous Lotka-Volterra system, see Brauer *et al.* (2000)[2]), where ω is the predator, λ is the prey, $\frac{\partial \phi}{\partial \lambda} > 0$, and, given equation (4), $\frac{\partial \kappa}{\partial \omega} < 0$ as soon as $\kappa(\cdot)$ increases. Figure 1 provides a typical diagram phase in the (ω, λ, d) space.

¹⁰See Appendix E for its calibration.

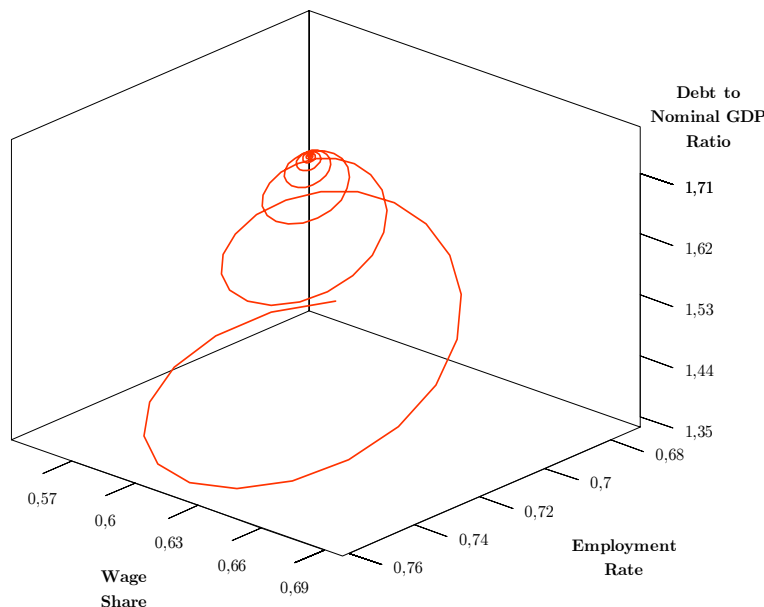


Figure 1: Phase diagram of employment rate *vs.* wage share and debt ratio in the exponential case.

As output grows, more workers are employed, hence the employment rate increases, which eases labor negotiations and, courtesy of the short-run Phillips curve (equation 6), induces an increase of the wage share, ω . As a result, inflation tends to accelerate (equation 6), which induces a positive backloop on wages as soon as workers do not share complete monetary illusion (i.e., $\gamma > 0$). As shown by equation 4, however, this process will devour the profit share, π , hence reducing investment (see equation 5). The slowdown of capital growth then results in a lower growth rate of output, reducing the growth rate of employment (remember equation 9). This reversal in trend cools down the wage growth rate, restoring the profit rate in the medium run and hindering cost-push inflation. Empirically estimated at the world level, this simplistic version of our model yields an endogenous cycle with a periodicity of 12-18 years – thus close to the Kuznets business swings (cf. Kuznets [27]). In the long run, however, the magnitude of each cycle shrinks, and the state of the economy converges towards a stationary state: while output still grows exponentially, the endogenous volatility of most parameters tends to zero, and a phenomenon akin to the “Great Moderation” occurs. The employment rate oscillates around 72%, and the wage share converges in the region of 0.62. At variance, however, with the celebrated Great Moderation observed in the decade preceding the global financial crises of 2007-2009, here, the economy converges to a *bona fide* long-run equilibrium since the debt-to-output ratio also stabilizes at around 1.71.

The main purpose of this paper is to understand how global warming will affect this basic cyclical interplay between real and monetary forces.

3 The climate module

This section presents the climate feedback on the economy, that is to say, CO₂ emissions, their impact on temperature, and the damage their build-up causes to real output.

This module is inspired by its analog in DICE (2013)[40].

3.1 CO₂ emissions

As in Nordhaus (2015)[39], global CO₂ emissions are the sum of two terms: (i) E_{ind} , the industrial emissions linked to the consumption of fossil energies and (ii) E_{land} , the land-use emissions:¹¹

$$E := E_{ind} + E_{land}.$$

Industrial emissions are endogenously determined and depend on the level of real output according to

$$E_{ind} := Y\sigma(1 - n),$$

where n is the emission-reduction rate consequent to abatement efforts, and σ is the emission intensity of the economy. The latter is assumed to behave according to the following dynamic:

$$\frac{\dot{\sigma}}{\sigma} := g_{\sigma}, \text{ with } \frac{\dot{g}_{\sigma}}{g_{\sigma}} := \delta_{g_{\sigma}},$$

where $\delta_{g_{\sigma}} < 0$. While the initial value of σ is empirically given by data, the initial value of g_{σ} and the calibration of $\delta_{g_{\sigma}}$ are set to ensure that $g_{\sigma} \simeq -0.95\%$ per year until 2100 and -0.87% up to 2200. The dynamics of n will be presented shortly.

Land-use emissions are given by an exogenous dynamic

$$\frac{\dot{E}_{land}}{E_{land}} := \delta_E,$$

with $\delta_E < 0$. As in Nordhaus (2013)[40], the calibration is based on results from the Fifth Assessment of the IPCC (2013)[51], which reports a 3 GtCO₂ per annum contribution of land-use changes.

3.2 CO₂ accumulation

The carbon cycle is modeled through the interaction between three layers in which total CO₂ emissions, E , accumulate: (i) the atmosphere (AT); (ii) a mixing reservoir in the upper ocean and the biosphere (UP) and; (iii) the deep ocean (LO). This mechanism is represented by the matrix system

$$\begin{pmatrix} \dot{\text{CO}}_2^{AT} \\ \dot{\text{CO}}_2^{UP} \\ \dot{\text{CO}}_2^{LO} \end{pmatrix} = \begin{pmatrix} E \\ 0 \\ 0 \end{pmatrix} + \underbrace{\begin{pmatrix} -\phi_{12} & \phi_{12} \frac{C_{ATeq}}{C_{UPeq}} & 0 \\ \phi_{12} & -\phi_{12} \frac{C_{ATeq}}{C_{UPeq}} - \phi_{23} & \phi_{23} \frac{C_{UPeq}}{C_{LOeq}} \\ 0 & \phi_{23} & -\phi_{23} \frac{C_{UPeq}}{C_{LOeq}} \end{pmatrix}}_{:=\Phi} \begin{pmatrix} \text{CO}_2^{AT} \\ \text{CO}_2^{UP} \\ \text{CO}_2^{LO} \end{pmatrix},$$

where E stands for the total CO₂ emissions, CO_2^i is the CO₂ concentration in layer $i \in \{AT, UP, LO\}$, ϕ_{ij} captures the CO₂ flow from layer i to layer j , and C_{ieq} is some

¹¹In concrete terms, this second term can be viewed as being induced by deforestation and the implied release of CO₂.

constant scaling parameter corresponding to the pre-industrial CO₂ equilibrium concentration on layer i .

At first, total emissions E are released into the atmospheric layer increasing its CO₂ concentration. Then, through diffusion and absorption phenomena, they spread between the other layers according to the matrix Φ . Note that each column of Φ sums to zero, meaning that the total CO₂ concentration in all three layers is accumulating at the rate of emissions E . As a result, assuming the atmospheric layer is the sole contributor to radiative forcing, the remaining layers act as sinks and mitigate temperature increase over time.¹²

3.3 Radiative forcing

The accumulation of greenhouse gases from anthropogenic sources induces a change, F , in global radiative forcing according to

$$F := F_{ind} + F_{exo},$$

where F_{ind} stands for the radiative forcing due to CO₂ accumulation (closely linked to industrial production, and projected to be the main contributor of global warming), and F_{exo} stands for an exogenous forcing capturing the impact of other long-lived greenhouse gases and other factors such as albedo changes or the cloud effect. According to the Representative Concentration Pathways (hereafter RCP) database provided by the Fifth Assessment of the IPCC (2013)[51], the effect of non-CO₂ radiative forcing is estimated to be lower than CO₂ radiative forcing. Therefore, following Nordhaus (2013)[40], exogenous forcing will be modeled by the dynamics

$$\dot{F}_{exo} = \delta_{F_{exo}} F_{exo} \left(1 - \frac{F_{exo}}{0.7}\right)$$

with $\delta_{F_{exo}} > 0$. In 2010, the exogenous forcing is calibrated at 0.25 W/m² and designed to grow smoothly in order to be close to 0.7 W/m² in 2100, in line with the RCP trajectories.

Industrial radiative forcing is defined as follows:

$$F_{ind}(t) = \frac{F_{2 \times CO_2}}{\log(2)} \log \left(\frac{C_{CO_2(t)}}{C_{CO_2(t_0)}} \right),$$

where F_{2CO_2} is the net radiative forcing associated with a doubling of atmospheric CO₂ concentration.

3.4 Temperature change

A change of radiative forcing induces a change, T , in the global mean atmospheric temperature. Following Geoffroy *et al.* (2013)[10], global thermal behavior is modeled through an energy-balance model of two coupled layers: (i) the atmosphere, land surface, and upper ocean, and (ii) the deeper ocean. In this framework, each layer obeys the following dynamic:

$$\begin{cases} C\dot{T} = F - (RF)T - \gamma^*(T - T_0) \\ C_0\dot{T}_0 = \gamma^*(T - T_0), \end{cases} \quad (12)$$

¹²The calibration of the matrix Φ is available in Appendix D.

where F is the radiative forcing, RF is the radiative feedback parameter, γ^* is the heat exchange coefficient, C is the heat capacity of the atmosphere, land surface and upper ocean layer, C_0 is the heat capacity of the deep ocean layer and T and T_0 are the mean temperature perturbation (deviation from the 1900 value) of respectively the atmosphere, land surface and upper ocean layer, and the deep ocean layer. The long-run equilibrium of the temperature anomaly is given by $T = F/RF$ and will control the climate sensitivity as in Dietz-Stern (2015)[6].¹³

3.5 Climatic damages

For our baseline scenario, we rely on the quadratic form of the damage function proposed by Nordhaus (2013)[39]:

$$\mathbf{D} = 1 - \frac{1}{1 + \pi_1 T + \pi_2 T^2},$$

with $\pi_1 = 0$, $\pi_2 = 2.84 \times 10^{-3}$. Initially, the function relied on various sectoral studies such as crop losses or change in energy demand for space cooling or heating for several points of global warming. It was then aggregated to describe the global impact of global warming based on the estimates of Tol (2009)[52]. This damage function is explicitly designed to model the effects of a global warming contained within a range of 0°C to 3°C. No threshold effects are thus allowed in this scenario after a temperature anomaly above 3°C.

3.6 Abatement costs

As public policy instruments are deployed, carbon emission abatement is achieved with a cost, GY , partly borne by investment at the rate μ .¹⁴ The ratio, G , of abatement cost to real output is defined by the following relation:

$$G = \theta_1 n^{\theta_2},$$

where n stands for the rate of emissions reduction, defined shortly, and $\theta_1, \theta_2 > 0$. Here, $\theta_2 > 0$ is calibrated so that the abatement-cost-to-output ratio is highly convex.

The dynamics of abatement costs is linked to a backstop technology with a price p_{BS} and able to replace carbon-intensive technology, and to a carbon price instrument p_C .¹⁵ These prices follow exogenous trajectories defined by

$$\frac{\dot{p}_{BS}}{p_{BS}} = \delta_{p_{BS}} < 0,$$

$$\frac{\dot{p}_C}{p_C} = \delta_{p_C} > 0.¹⁶$$

¹³The calibration of the system (12) is available in Appendix B.

¹⁴For the sake of completeness, the remaining part, $(1 - \mu)$, is borne by households.

¹⁵This price refers to the price per ton of CO₂.

¹⁶A sensitivity analysis will be provided. First, we use the same baseline as in Nordhaus *et al.* (2013)[40]. The next scenarios, based on Nordhaus *et al.* (2013)[40] and Dietz and Stern (2015)[6], will be calibrated so that the growth parameter δ_{p_C} and the initial value of P_C is in line with the optimal values reported in 2020 and 2050 (resp. 2015 and 2055), defined shortly.

The reduction rate reflects an arbitrage relation between the relative prices of carbon and of the backstop technologies respectively,

$$n := \min \left\{ \left(\frac{p_c}{p_{BS}} \right)^{\frac{1}{\theta_2 - 1}} ; 1 \right\}.$$

The parameter, θ_1 , reflects the cost of investing in the backstop technology through its price and the carbon intensity of the economy. The parameters θ_1, θ_2 are calibrated according to Nordhaus (2013)[40]. Whenever $p_c \geq p_{BS}$, the energy shift is completed.

Having described all the ingredients of our model, we are now ready to analyze the scenarios resulting from the interaction between global warming and debt accumulation.

4 Scenarios

Using the calibration depicted *supra*, we are now ready to discuss four main classes of narratives that depend on labor productivity growth scenarios and previously defined damage functions. The baseline case, the influence of each specification, and finally some combinations are successively analyzed. For each scenario, the initial point is the year 2010 and the simulations run until 2300, unless a collapse occurs before the final model period.

4.1 Exponential technological progress

For the baseline case, we begin with an exogenous technological progress dynamic. Labor productivity is assumed to grow at a constant rate:

$$\frac{\dot{a}}{a} := \alpha > 0. \tag{13}$$

For our simulations, we shall adopt two values for α : either 0.0226 or 0.015. The first is based on an observed trend of technological progress at the world level.¹⁷ The second is a proxy of the parameterization adopted in Nordhaus (2013)[40]. Table 2 presents the main parameters of our baseline simulation, obtained in the “exponential case” $\alpha = 0.0226$, as specified in Appendix (E.2). Monetary values are in US\$ trillions. The population size is in billions. The GDP deflator (price level) is normalized to 1 in 2010. As already said, the short-run interest rate, r , is kept constant at 3%.

Parameter	Y_{2010}	N_{2010}	ω_{2010}	λ_{2010}	d_{2010}	p_{2010}	α
Value	64.4565	4.5510	0.5849	0.6910	1.4393	1	0.0226

Table 2: Main macroeconomic parameters of the exponential case

Figure 2 presents the deterministic exponential trajectories of our main macroeconomic and climate variables. After some fluctuations, the world economy reaches a stable path with a finite debt ratio and stable inflation (roughly 2%). Yet, due to high emissions of CO₂ (up to approximately 147.34 Gt CO₂ in 2100), the temperature increases

¹⁷See details in Appendix E.2.

(3.95°C in 2100 in the atmospheric layer) and thus augments damages to production. As a consequence, in the (ω, λ, d) -space represented in Figure 4, the wage share, ω , and the employment rate, λ , slowly decrease. Then, as the energy shift reaches completion a little before 2250, CO₂ concentration, and thus damages, decrease.

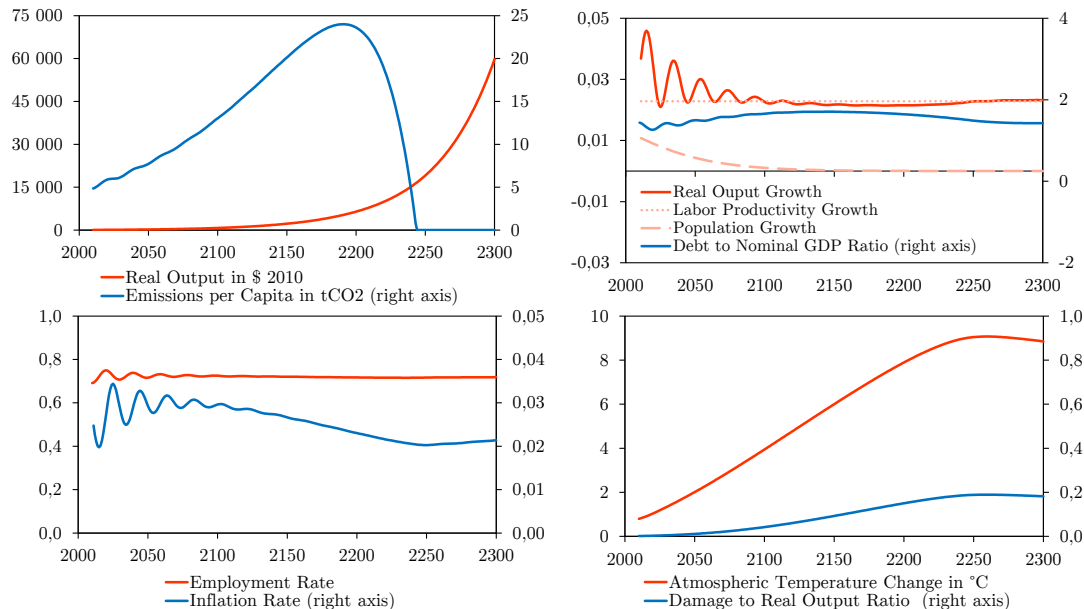


Figure 2: Trajectories of the main simulation outputs in the exponential case.

This baseline scenario yields important takeaways. First, as could be expected, deterministic exponential productivity growth successfully drives the exponential growth of real GDP, despite climate damages. In 2100, it reaches 11.5 times its initial volume in 2010. This uninterrupted growth is accompanied by monetary and real cycles with a periodicity of 12-17 years. This is consistent with the celebrated Kuznets swings, which have been recently re-examined by Korotayev and Tsirel (2010)[26]. However, as time passes, these cycles seem to shorten during the first half of the twenty-second century. Ultimately, all volatility vanishes. Such a secular “Great Moderation” means that the global dynamical system is converging towards a long-run equilibrium where the employment rate stabilizes around a comfortable 72% ratio, while the real output growth rate converges slightly above 2%. The (private nonfinancial corporate) debt-to-GDP ratio reaches a maximum in the middle of the twenty-second century (around 1.7) before declining towards 142%.

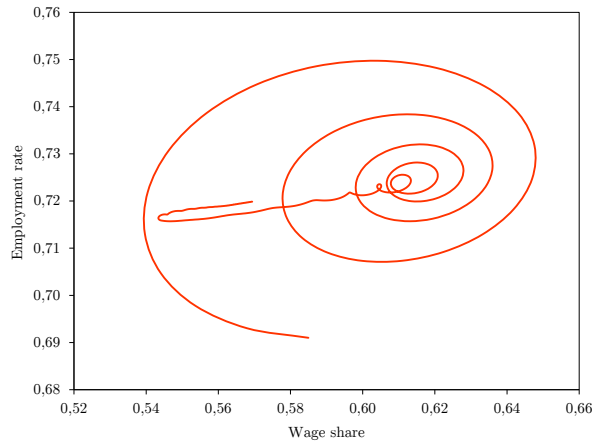


Figure 3: Phase diagram of employment rate vs. wage share in the exponential case over the period 2010-2900.

As a consequence of the rise in CO_2 concentration, the state of the world economy, illustrated by the phase portrait (ω, λ) in Figure 3, first deviates from its long-run equilibrium point. This temporary deviation reflects the impact of damages on the long-run equilibrium and especially on the wage share. Indeed, from 2100 until the energy shift is completed, the rise in damage, $\dot{\mathbf{D}}$, is at its highest. At the same time, the wage share declines in line with equation 10; so does inflation. Hence, higher profits lead the debt ratio to stagnate before declining. In the aftermath of the transition to clean energy, the private debt-to-GDP ratio stagnates towards a long-run equilibrium level while damages start a downward-sloping trend.

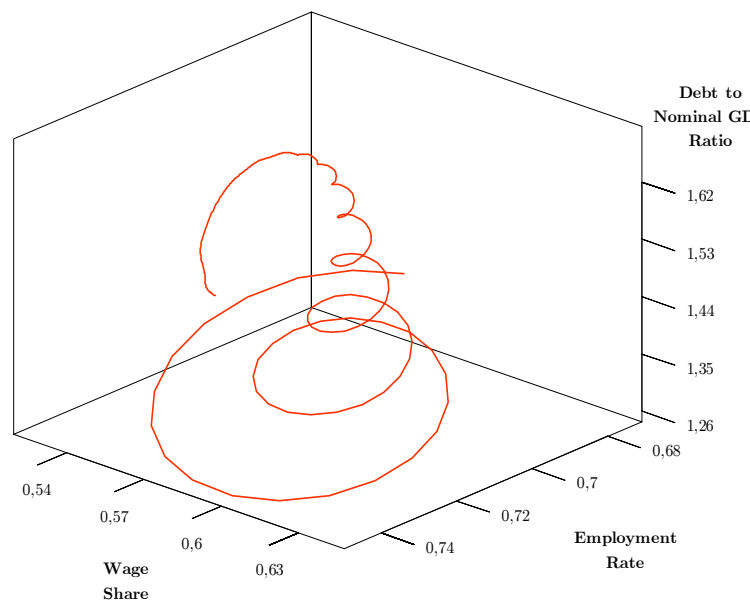


Figure 4: Phase diagram of employment rate vs. wage share and debt ratio in the exponential case.

As shown by the three-dimensional phase diagram in Figure 4, the (ω, λ) -plane first converges towards some equilibrium point close to $(0.61, 0.72)$. But, soon after 2150, the

wage share shifts towards 0.55. This departure from the long-run stationary state of the world economy is only temporary, and entirely caused by climate change. Indeed, further simulations up to the year 2900 presented in Figure 3 show that, from the twenty-fourth century on, the state of the economy slowly reverts to the long-term equilibrium just alluded to.

This first scenario offers a quite reassuring picture in the time scale of the century. By 2050, as shown in Table 3, the average yearly CO₂ emission per capita is 7.72t. The temperature change in 2100 is +3.94°C and CO₂ concentration, 968.98 ppm. Despite the fact that we are far above the goal unanimously adopted at the Paris Agreement in 2015, the world economy is going pretty well: the damages induced by global warming reduce the final world real GDP by one fifth – a fraction higher than the 5% losses first envisaged by Stern (2006)[48] but this is seemingly easily counterbalanced by the strength of the postulated exogenous growth. As a result of this quite unrealistic picture, CO₂ emissions peak only in the middle of the twenty-second century and the zero-emission level is reached one century later!

GDP Real Growth 2100 (wrt 2010)	1053%
t CO ₂ per capita (2050)	7.72
Temperature change in 2100	+3.94 °C
CO ₂ concentration 2100	968.98 ppm

Table 3: Key values of the world economy by 2100 – the exogenous case.

By exhibiting a relatively low impact of damages and negligible abatement costs (less than 1% of real output) for production by 2100 or so, this scenario above all confirms the unrealistic feature of the climate-economy interaction modeling on which it is based. As we shall now see, the picture changes dramatically as soon as labor productivity is made endogenous.¹⁸

4.2 Endogenous productivity

Let us now discuss alternative scenarios of endogenous labor productivity growth combined with the damage function introduced by Nordhaus (2013)[40].

4.2.1 The Kaldor-Verdoorn case

The Kaldor-Verdoorn case assumes a relationship between labor productivity growth and output growth (cf. Verdoorn (2002)[56]) in the form

$$\frac{\dot{a}}{a} := \alpha + \eta g, \tag{14}$$

with g being the real output growth, and $\alpha, \eta > 0$. Equation 14 can be interpreted as reflecting dynamic economies of scale (or “learning by doing”). A rough estimate for the United States over the last four decades is $\alpha \simeq 0$ and $\eta \simeq 0.5$, with a tendency

¹⁸For the sake of comparison with DICE, the “Nordhaus scenario”, and Gordon (2014)[16] – where labor productivity grows approximately at the deterministic pace of 1.5% and 1.3% respectively – are discussed in [the supplementary web material](#). The findings are qualitatively similar to the ones just described.

of both parameters to increase due to the impact of Information and Communication Technologies. In our simulations, we assume equation 14 to hold at the world level. This will be considered optimistic or pessimistic depending on how strongly one believes that the opportunity for emerging economies to follow a learning process analogous to the recent trend in the United States is realistic or not.

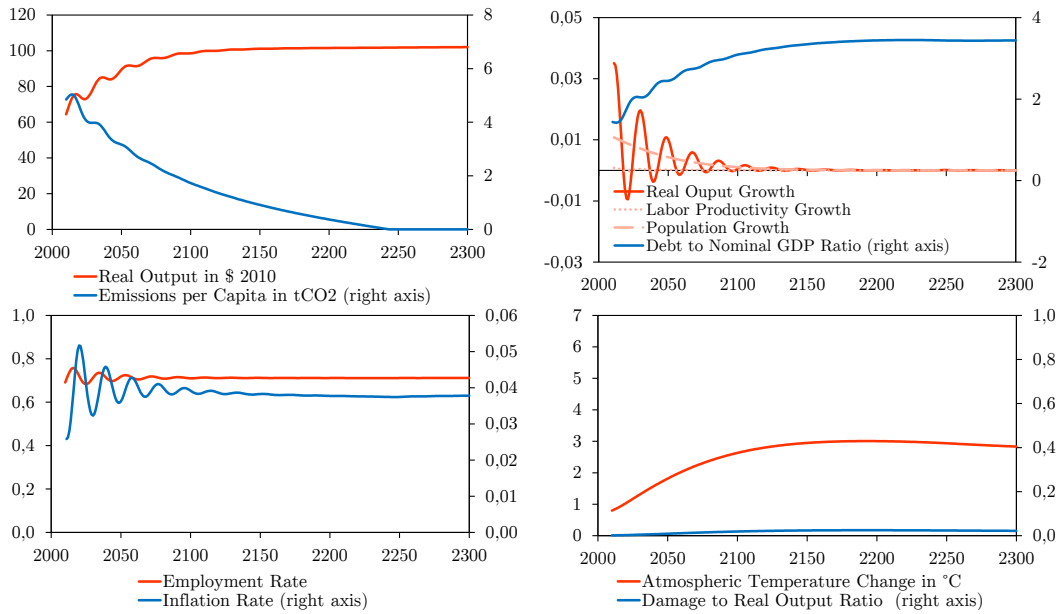


Figure 5: Trajectories in the Kaldor-Verdoorn/Nordhaus case.

Figure 5 depicts the path followed by the world economy in the Kaldor-Verdoorn scenario. By contrast with the previous pattern, the economy converges to a stationary state with stagnating labor productivity and no real output growth. This “millennial stagnation” starts at the end of this century and is accompanied by a debt ratio and inflation rate higher than in the exponential case. Carbon emissions decline almost immediately after 2010. The zero emission floor is reached before the second half of the twenty-second century.

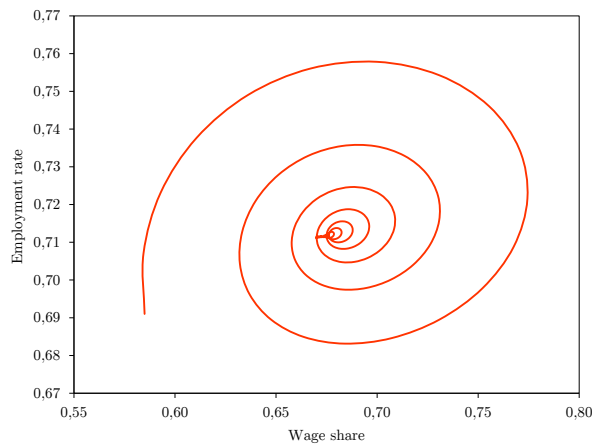


Figure 6: Phase diagram of employment rate vs. wage share in the Kaldor-Verdoorn/Nordhaus case.

Again, the almost negligible damage inflicted by global warming on the world economy, despite the fact that the average temperature change reaches approximately $+2.63^\circ$ or so by the end of this century, casts serious doubts on the realism of the damage function. This thought experiment, however, reveals that, if all the parameters of the economy are kept as before and technological progress is made to depend on growth itself, this suffices to break with the “infinite growth” story and leads to long-run economic stagnation.

The key variables characterizing the world situation by the end of this century are summarized in Table 4:

GDP Real Growth 2100 (wrt 2010)	53%
t CO ₂ per capita (2050)	3.17
Temperature change in 2100	+2.63 °C
CO ₂ concentration 2100	521.094 ppm

Table 4: Key values of the world economy by 2100 – the exogenous case.

4.2.2 The Burke *et al.* (2015) case

This scenario allows for time-varying labor productivity that adapts endogenously to temperature anomaly. In Burke *et al.* (2015)[3], a comprehensive econometric model of the dependency of world GDP growth on climate parameters is provided. In particular, a quadratic relationship between the mean annual temperature and income growth is introduced, from which we deduce the following relation between labor productivity and atmospheric temperature:

$$\frac{\dot{a}}{a} := \alpha_1 T_a + \alpha_2 T_a^2,$$

where T_a stands for the absolute atmospheric temperature and α_1, α_2 are estimated by Burke *et al.* (2015)[3]. Their article provides a range of seventeen models of regression.¹⁹ We selected their most general specification²⁰ based on GDP growth data from the Penn World Tables in order to be in line with our own data sources. This calibration leads to $\alpha_1 \simeq 0.0072$ and $\alpha_2 \simeq -0.0004$.

Figure 7 shows first an increase and then, around 2150, a severe loss of labor productivity due to its nonlinear relationship with the absolute value of atmospheric temperature. Hence, as the change of temperature in the atmospheric layer exceeds approximately 4°C , labor productivity peaks in the region of this threshold, and real output starts decreasing. As a result, the world productive sector is forced to leverage in order to finance investment, such that the debt-to-output ratio increases twice as fast compared with the previous scenario. This failure of technological progress to fuel growth induces a delay in the private sector’s deleveraging process, which results in a degrowth of real output

¹⁹Burke *et al.* (2015)[3] implement a first-difference panel regression assessing a quadratic temperature impact on GDP growth with fixed effects on countries and periods, flexible country-specific trends and precipitation controls (quadratic impact). Their methodology is robust and copes with both observed and unobserved effects such as nonlinear country-specific demographic trends. They propose a range of seventeen models of regression studying several samples, an additional explanatory variable (developed and developing countries), and an alternative data source (the Penn World Tables, while their main source is the World Bank).

²⁰We mean by “most general specification” the estimation realized on the full sample without an additional explanatory variable of the developed/developing country criteria.

starting in the second half of the twenty-second century. In the vicinity of the model year 2135, world real GDP peaks at around 600% of its 2010 value, and then inexorably declines. As a counterpart, the debt-to-GDP ratio explodes: it is already above 250% by 2100, and peaks slightly below 400% thereafter. Fortunately, emissions per capita have already peaked around 2050, such that the temperature change in 2100 remains lower than in the exogenous-growth scenario (+4.92°C).

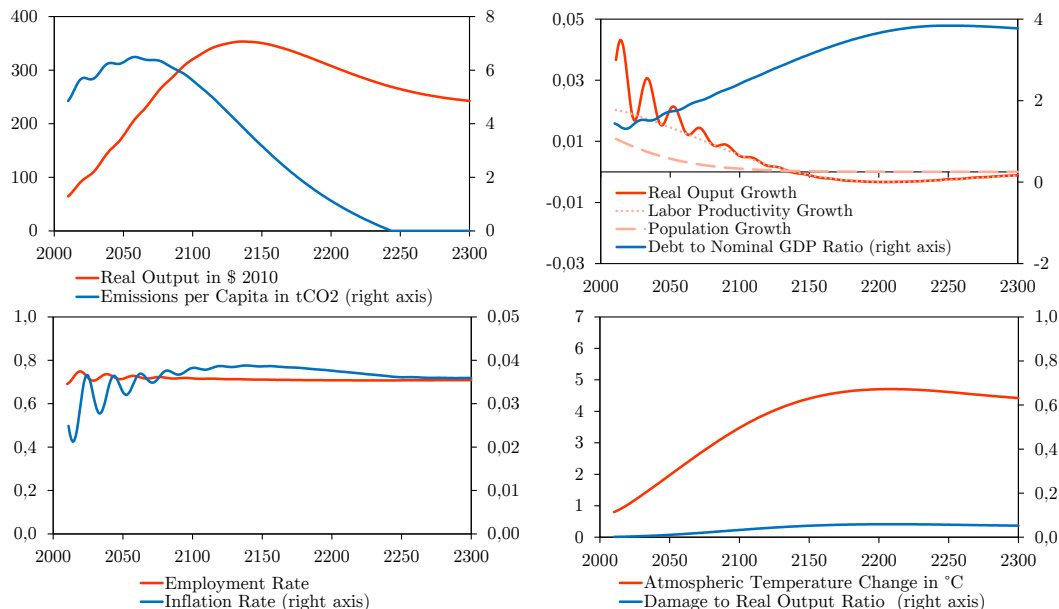


Figure 7: The Burke *et al.* labor productivity trajectory with the Nordhaus damage function.

The phase diagram in Figure 8 highlights the channel linking global warming, surplus distribution, and growth. Indeed, as a consequence of equation 10, the deceleration of labor productivity favors an increase in the wage share, lowering relative profits and forcing the private sector to increase its debt in order to compensate for profit losses.

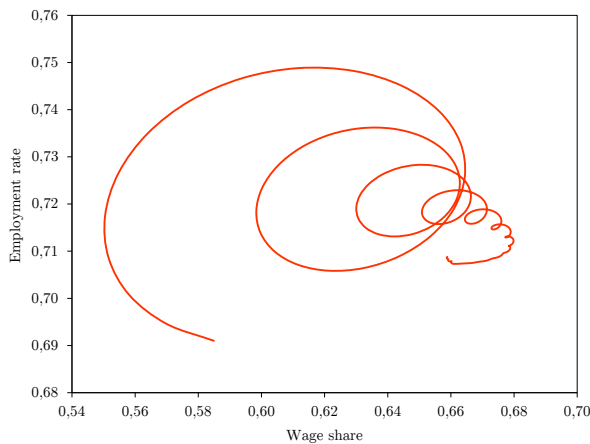


Figure 8: Phase diagram in the Burke *et al.*/Nordhaus case.

However, this “degrowth by constraint” (not by design) has no disruptive effect on the labor market, since the employment rate converges around 70% at the end of this

century. As for inflation, this is slightly higher than in the previous scenario but eventually converges to a quite reasonable 3.5% in the second half of the twenty-third century. Notice also that the damage function has very little impact in this scenario, as in the previous one, since the temperature anomaly peaks at around only 3.5°C or so.

GDP Real Growth 2100 (wrt 2010)	397%
t CO ₂ per capita in 2050	6.29
Temperature change in 2100	+3.48 °C
CO ₂ concentration in 2100	744.49 ppm

Table 5: The world economy by 2100 – the endogenous case with Nordhaus damage function.

Of course, forced degrowth at the world scale might seem an implausible pattern given the impressively innovative character of advanced economies (think of the ICT revolution) and the quite impressive growth experienced by emerging countries in recent decades. Remember, however, that during the 1990s the former Soviet Union experienced a 50% reduction of its GDP within one decade, while Greece lost 25% of its GDP between 2010 and 2015. Undesired degrowth is not therefore a fictional phenomenon.

Thus far, we have kept the damage function identical and discussed the sensitivity of our prospective paths with respect to various specifications of technological progress. Let us now proceed the other way round and test various damage functions while keeping a deterministic exponential labor productivity growth.

4.3 Assessing the impact of climate change

So far, there is no academic consensus on a functional formulation and calibration of the damage function capturing the impact of climate on the world economy. Indeed, as pointed out by Pindyck (2015)[41], no theory and no data exist on which such a consensus could be reliably grounded. On the other hand, this function has to summarize the economic impacts, as a percentage of output, brought on by the rise in mean atmospheric temperature. It thus has to compile a wide range of events such as biodiversity loss, ocean acidification, sea-level rise, change in ocean circulation, and high-frequency storms, among others. As a consequence, the damage function is highly nonlinear with threshold effects. In this section, various damage functions will be considered. We keep labor productivity at the somewhat high growth rate of 2.26%, so that the only difference with the BAU scenario analyzed *supra* lies in our assessment of climatic damages.

As argued by Dietz and Stern (2015)[6], Nordhaus' quadratic form leads to unrealistically low damages beyond a temperature increase of 4°C. For instance, a global warming of 4°C would lead to only 4% of output loss whereas, according to natural science and economic studies, reaching this threshold could be a milestone. On the one hand, Lenton *et al.* (2008)[28] point out that several key tipping points in the climate system could be crossed and lead to severe impacts on the natural environment. On the other hand, Stern (2013)[49] shows that this situation would generate large migrations associated with conflict and loss of life. Our simulations in the next section will unfortunately confirm this criticism.

As a result, and in line with Pindyck[41], we adopt the educated guess provided by Dietz and Stern (2015)[6] with a polynomial damage function

$$D = 1 - \frac{1}{1 + \pi_1 T + \pi_2 T^2 + \pi_3 T^{6.754}},$$

based on what Nordhaus proposes (same coefficients for the linear and quadratic parts). More precisely, the Weitzman function corresponds to $\pi_1 = 0$, $\pi_2 = 2.84 \times 10^{-3}$, and $\pi_3 = 5.070 \times 10^{-6}$, while the Dietz-Stern function yields $\pi_1 = 0$, $\pi_2 = 2.84 \times 10^{-3}$, and $\pi_3 = 8.19 \times 10^{-5}$.

The calibration proposed by Weitzman (2012)[58] leads to damages equal to 50% of output with a temperature increase of 6°C. That suggested by Dietz and Stern (2015)[6] yields damages equal to 50% of output with a temperature increase of 4°C. As emphasized by Weitzman (2012)[58] quoting Sherwood and Huber (2010)[45], given that a temperature increase of 12°C would exceed the human limits to metabolic heat dissipation, these educated guesses see relatively credible.

Figure 9 presents the shapes of the different damage functions considered in this study. One can observe the common pattern for Nordhaus' and Weitzman's specifications in a global warming ranging between 0°C and 3°C.

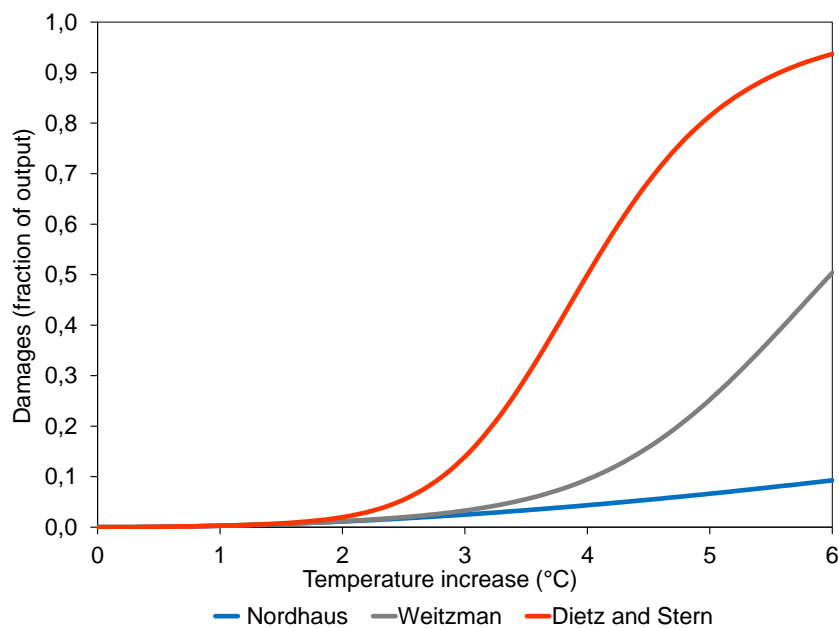


Figure 9: Shape of damage functions.

4.3.1 The Weitzman damage function

Figure 10 shows the trajectories of the world economy in the Weitzman damage function case. Here, the damage function drags the wage share to lower levels, leading the inflation rate towards negative values. Despite its slowdown, output growth remains positive along the trajectory. By the end of the twenty-second century, the world's real output growth rate bottoms out at -2%, then starts to increase again. As shown by the bottom right quadrant of Figure 10, this is clearly due to the run-up of the impact of warming with respect to production, which mainly occurs during the twenty-second century. On the

other hand, the wage share, ω , stays below 35% until the end of the same century, implying high profits and the beginning of an age of deleveraging and even excess saving.²¹

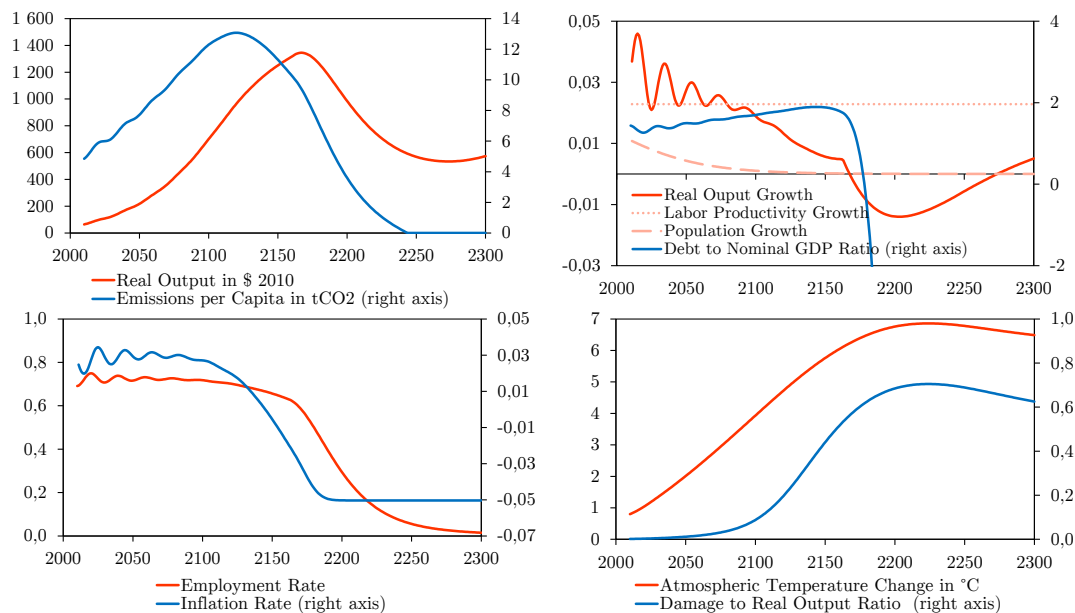


Figure 10: Trajectories of the main simulation outputs in the exponential/Weitzman case.

The phase portrait in Figure 11 highlights the decline of the wage share, while the employment rate steadily decreases to around 0. The fact that the world economy manages to produce some positive output growth in the second half of the twenty-third century, even though its employment rate is close to nil, confirms the unrealistic feature of our postulated exogenous growth rate of labor productivity.

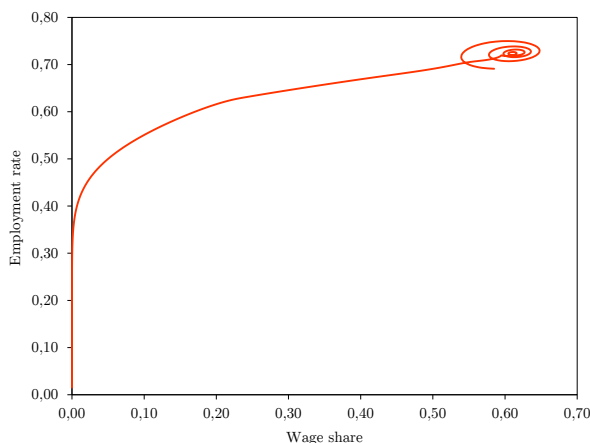


Figure 11: Phase diagram of employment rate vs. wage share in the exponential/Weitzman case.

²¹It is worth mentioning that the empirical estimation of investment, $\kappa(\cdot)$, as a function of the profit rate, π , is silent about domains where π has so far not been observed. This hardly surprising: climate change will necessarily lead the world economy to explore situations for which no data can be borrowed from the past. It does however raise a question: which values should be given to investment when π is abnormally high or low? Here, we have capped and floored $\kappa(\cdot)$ between 50% and 4% of real output.

GDP Real Growth 2100 (wrt 2010)	987%
t CO ₂ per capita in 2050	7.72
Temperature change in 2100	+3.93 °C
CO ₂ concentration in 2100	958.17 ppm

Table 6: The world economy by 2100 – the exogenous case with Weitzman damages.

4.3.2 Damages à la Dietz-Stern

Let us now adopt the probably more realistic Dietz-Stern damage function. Figure 12 shows its impact on the main macroeconomic and climate variables. Qualitatively, the short run exhibits a pattern similar to the previous scenario. Quantitatively, real GDP is more muted. In the previous scenario, it peaked in the region of (2010) US\$ 1400 trillion around 2175, whereas in the current scenario the highest point is reached in 2100 at slightly above US\$ 400 trillion. This more severe picture leads to a real GDP that is lower in 2175 than in 2010. In this scenario, damages absorb more than 60% of real output as the temperature increase in the upper atmosphere reaches 4°C around 2125. For the sake of comparison, at that date in the previous scenario “only” 20% of the world’s real output was destroyed by global warming. Finally, the debt-to-GDP ratio spikes at around 250% towards 2125, whereas in the Weitzman case it stood below 200% for the same period. A more severe damage function reinforces the run-up to debt during the period when the economy is still growing. Note that, as previously, a deleveraging period starts whenever GDP decreases.

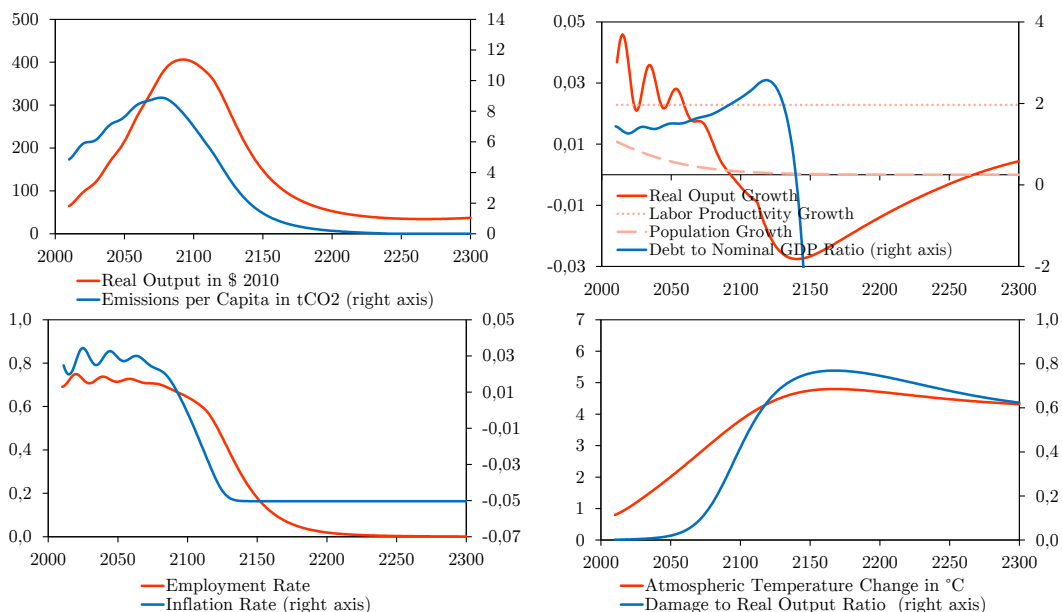


Figure 12: The exponential/Dietz-Stern case.

GDP Real Growth 2100 (wrt 2010)	520%
t CO ₂ per capita in 2050	7.63
Temperature change in 2100	+3.81 °C
CO ₂ concentration in 2100	857.19 ppm

Table 7: The world economy by 2100 – the exogenous case with the Dietz-Stern damage function.

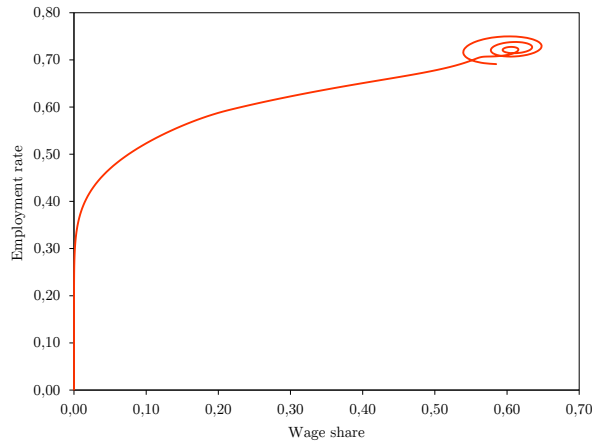


Figure 13: Phase diagram of employment rate vs. wage share in the Dietz-Stern/Nordhaus case.

4.4 Extreme climate change

In this subsection, we consider the scenarios resulting from the combination of endogenous technological progress and various damage functions.

4.4.1 The Burke *et al.* (2015)/Dietz-Stern case

Let us first combine endogenous labor productivity, non-linearly affected by climate change as described earlier (Burke *et al.* (2015)[3]), with a highly convex Dietz-Stern damage function. This time, as shown in Figure 14, although the temperature increase does not exceed 4°C, the combined effects of damages and loss of labor productivity lead to a planetary collapse around 2180, preceded by severe debt-deflation. As a consequence of the depressive effect of deflation and the subsequent breakdown of the world economy, the peak of CO₂ emissions is lower than in most of the previous scenarios, and occurs around 2080. Yet, due to the inertia effects of global warming, this early peaking cannot prevent a planetary collapse one century later.

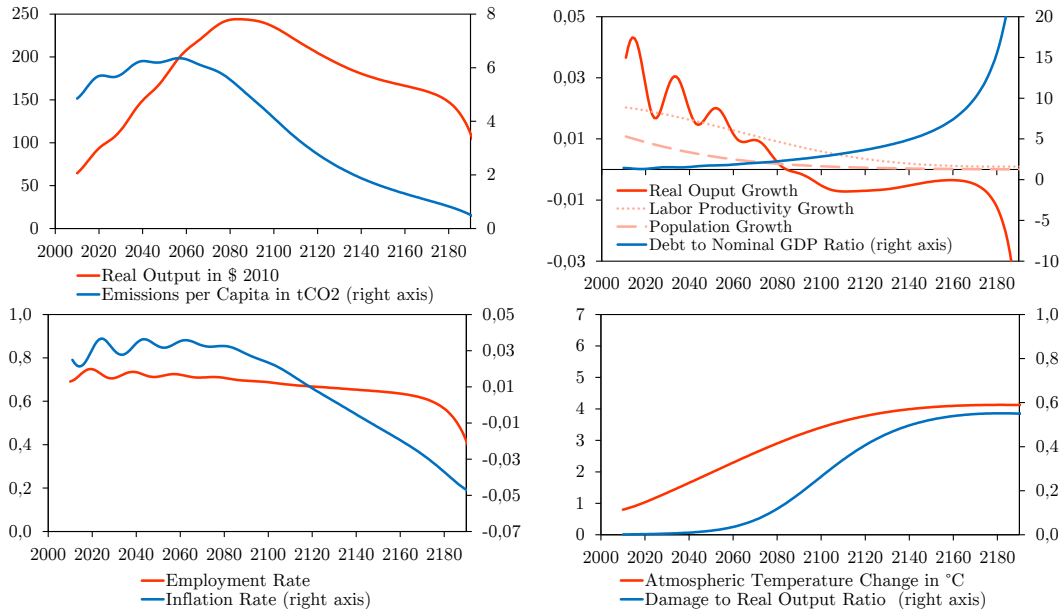


Figure 14: The Burke *et al.* (2015)/Dietz-Stern case.

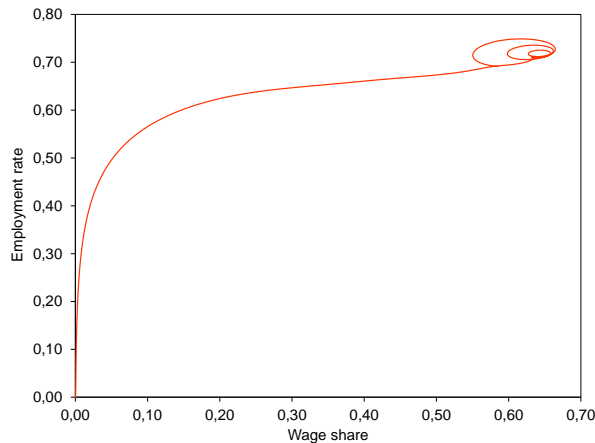


Figure 15: Phase diagram of employment rate vs. wage share in the Burke *et al.*/Dietz-Stern case.

4.4.2 The Burke *et al.* (2015)/Dietz-Stern case with a slower demographic trend

Could a deceleration of the demographic trend prevent a disaster? This subsection provides some elements for an answer by assuming the demographic trend to be slower than in the UN median scenario within the Burke *et al.* labor productivity growth case, together with the Dietz-Stern damage function previously presented. For this purpose, we divide by four the speed of convergence, q , but we keep the same upper bound for the dynamics of the labor force, M . Figure 16 offers a comparison of the demographic scenarios.

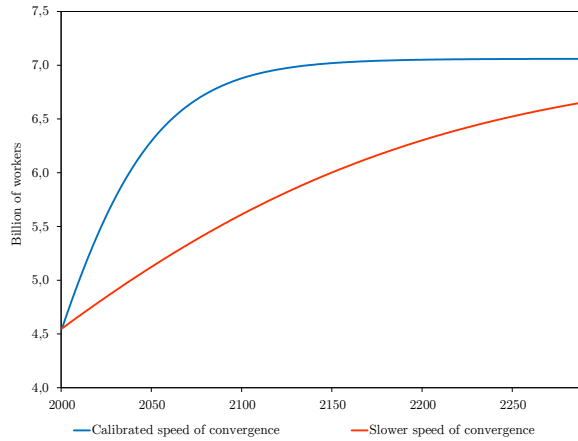


Figure 16: Comparison of the labor-force demographic trajectories.

According to our altered demographic scenario, the world’s working-age population would be approximately 5 billion people in 2100, instead of 7 billion as in the UN median projection. Figure 17 shows the paths followed by the world economy in this case. Despite lower CO₂ emissions, we observe patterns analogous to those obtained in the original Burke/Dietz-Stern case, leading to a global collapse around the model year 2240. The main difference between the two narratives lies in the speed at which events occur: the second narrative exhibits a 4–5-decade delay relative to the first. This suggests that a downturn in the demographic trend does not suffice *per se* to avoid a disaster, but it nevertheless manages to postpone it for a few decades.

Unfortunately, other simulations, even with no population growth,²² show that in the Burke/Dietz-Stern case a global collapse *always* occurs whatever the population trend. Even in the utterly unrealistic case in which world population stays at its 2010 level, the intrinsic devastating forces arising from the combination of climate change and debt would lead to a breakdown around 2400. In terms of public policy, this means that steering world population growth cannot be viewed as a panacea, but it *does* have a positive impact on the global economic calendar of our planet.

²²These simulations are available from the authors upon request.

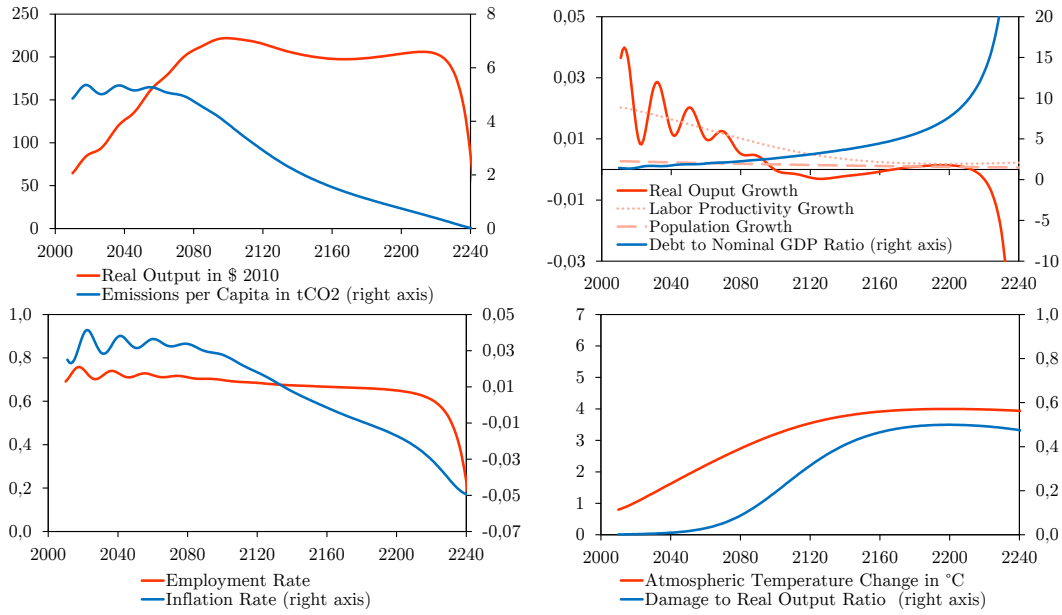


Figure 17: Trajectories of the main simulation outputs for the case with the Burke *et al.* (2015) labor productivity growth, a Dietz-Stern damage function, and a slower demographic trend.

4.5 Carbon prices and climate sensitivity

Since demography alone does not suffice to circumvent the potentially disastrous effects of global warming, we now turn to the carbon value. So far, we have considered the baseline scenario of the carbon price introduced by Nordhaus (2013)[40]. For the sake of clarity, the price of the t/CO_2 in (2005) \$US is one in 2010 and grows steadily by two percent per year.

In this section, we retain the Burke *et al.* (2015)[3] labor productivity dynamic coupled with a Dietz-Stern damage function, but modify the carbon price path, taking inspiration from Dietz and Stern (2015)[6]. On the demographic side, we again adopt the UN median projection, as we do throughout this paper except for Section 4.4.2 above.

4.5.1 Dietz and Stern's standard-run

We now assume that the carbon price follows the path examined in Dietz and Stern (2015)[6], starting with (2005) \$US 12 t/CO_2 in 2015 and reaching \$US 29 t/CO_2 in 2055.

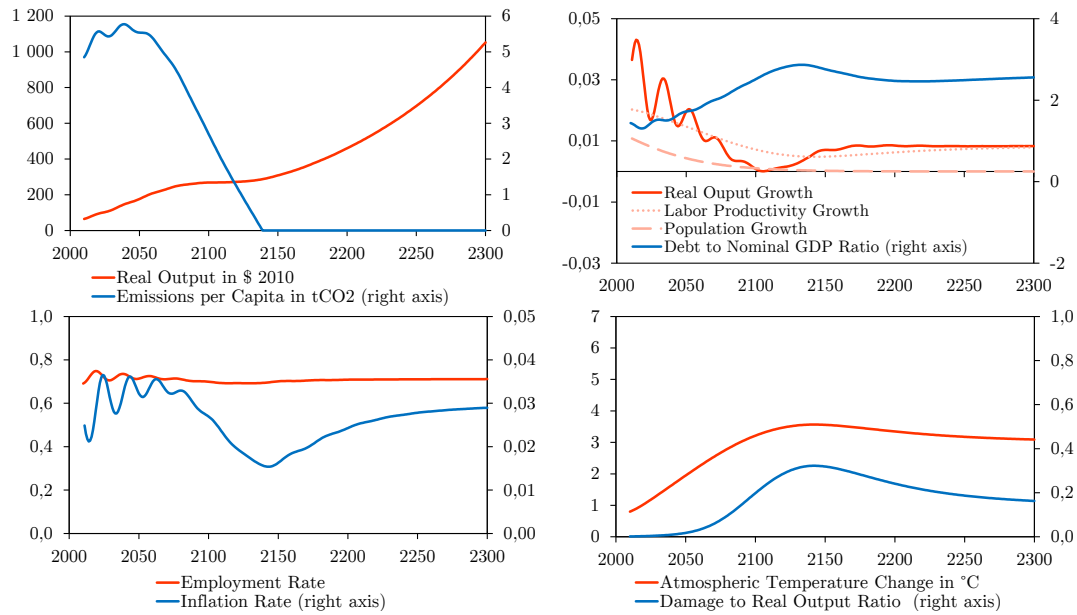


Figure 18: Trajectories in the Burke *et al.* (2015)/Dietz-Stern case with Stern’s standard-run carbon price.

Figure 18 shows that Stern’s carbon price path suffices to avoid the collapse. The higher carbon price prevents the +4°C temperature anomaly from being reached. As a result, damages are mitigated and, courtesy of the wage share dynamic, private debt remains at a reasonable level (less than 300%).

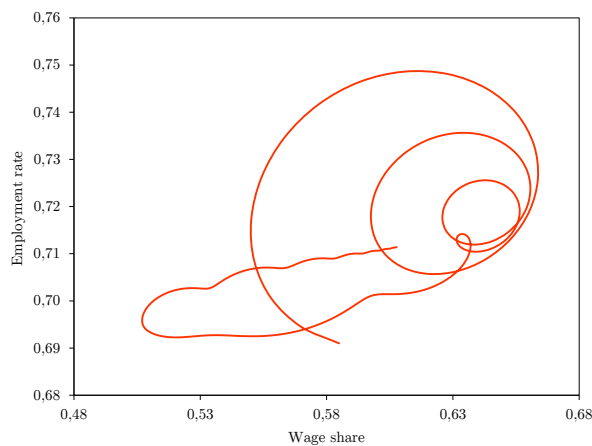


Figure 19: Phase diagram of employment rate vs. wage share in the Burke *et al.*/Dietz-Stern case with Stern’s carbon price path.

Figure 19 shows how the (ω, λ) -point converges towards long-run equilibrium. In this phase portrait, we can observe the mixed effect on the wage share of both the damage function that is driving the wage share down and the decreasing labor productivity that alleviates the slowdown.

Obviously, increasing the carbon price emerges as a viable solution to the economic side of the climate change problem – even though not every carbon price path successfully accomplishes this task. One should note, however, that this success is clearly due to the

utterly simple, and probably unrealistic, way we model the world economy’s shift from a current energy mix comprising 80% of fossil energies towards a zero-carbon economy.

4.5.2 Dietz and Stern’s standard-run with a climate Sensitivity of 6

So far, all our results are based on a climate sensitivity whereby a doubling in the atmospheric concentration of CO₂ translates into a +2.9°C rise relative to the pre-industrial era. This value reflects the mean of a Pareto distribution whose tail yields a 6% likelihood that a rise of +6°C or more will occur in these circumstances (see Weitzman (2011)[57]). We thus test some of our scenarios under a climate sensitivity of 6, rather than 2.9. Clearly, in this setting, any variation of CO₂ will lead to a higher response in temperature anomaly compared to its +2.9°C counterpart.

We begin with the most problematic scenario examined thus far, namely that in subsection 4.4.1 *supra*, which combines an endogenous labor productivity *à la* Burke *et al.*(2015) and a highly convex Dietz-Stern damage function. At variance with the situation envisaged in the subsection just mentioned, here, we keep the carbon price path introduced by Stern (instead of relying on Nordhaus’s price path as in section 4.4.1).

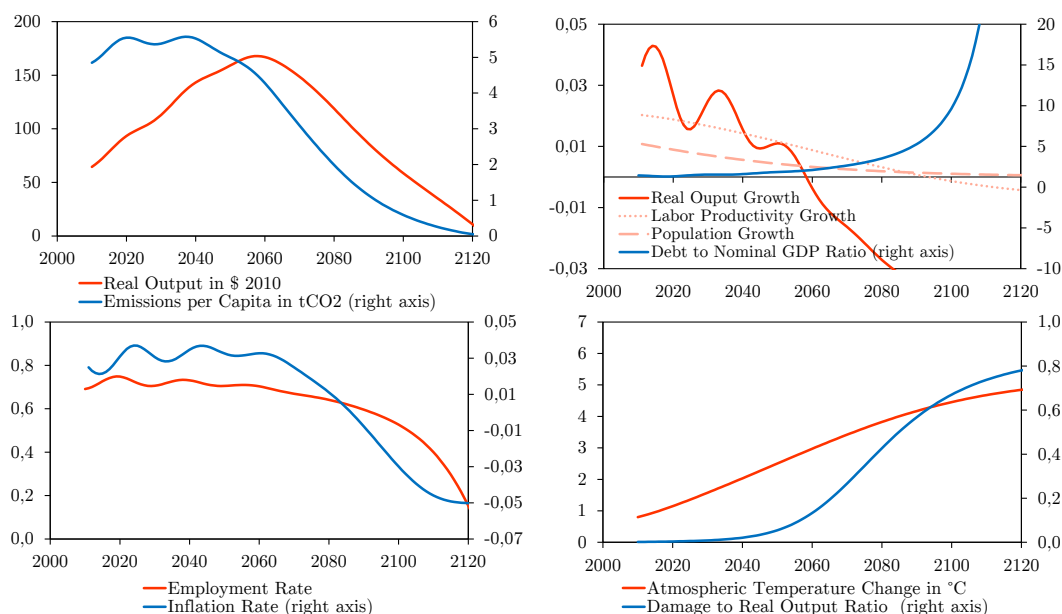


Figure 20: Trajectories in the Burke *et al.* (2015)/Dietz-Stern case with the standard-run price of carbon and a climate sensitivity of 6.

Figure 20 shows that the preceding specification of the carbon price no longer avoids a collapse of the economy. The cap of a +4°C temperature rise relative to the pre-industrial level is reached long before 2100. Consequently, high damages together with the inertia of CO₂ in the atmospheric layer lead the world economy to deflation and a skyrocketing debt ratio, yet again ending up in a global breakdown.

Next, we test the carbon price path more recently introduced by Dietz and Stern (2015)[6] for a climate sensitivity of 6 and a damage function *à la* Weitzman. Converted into 2005 \$US, in 2015 the price of the ton of CO₂ is now US\$ 74, and US\$ 306 in 2055.

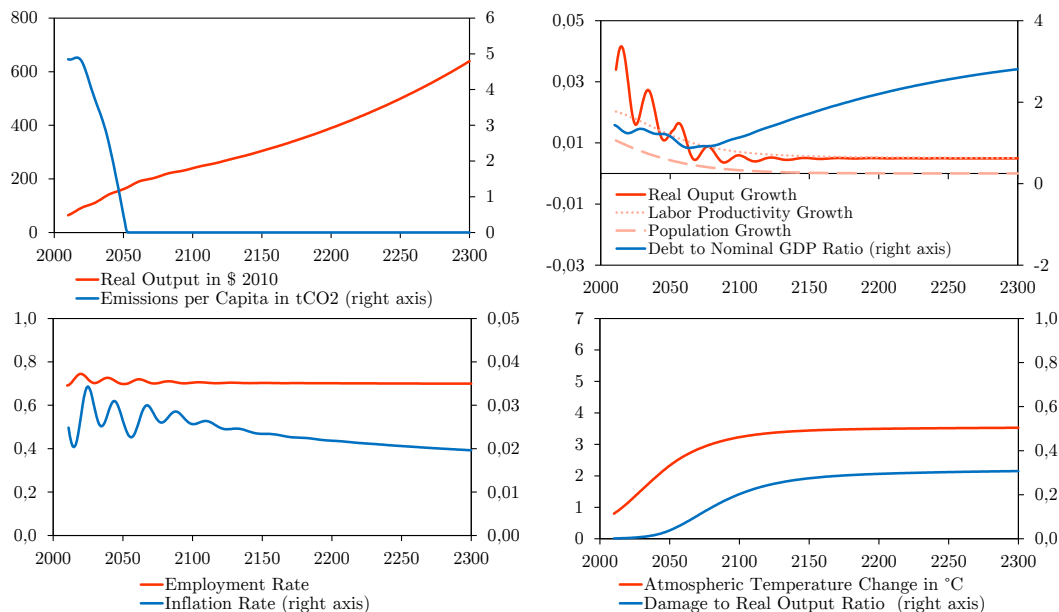


Figure 21: Trajectories in the Burke *et al.* (2015)/Dietz-Stern case, the Dietz-Stern carbon price path, and a climate sensitivity of 6.

This time, the carbon price path turns out to be sufficient to avoid the collapse. Figure 21 displays a trajectory in which real GDP in 2100 reaches about 2.72 times its value in 2010, with the emission of t CO₂ per capita decreasing to 0.70 in 2050 and the temperature increasing to only +3.23°C in 2100.

4.5.3 Objective +1.5°C

The Paris Agreement of 2015 aims to keep the temperature anomaly below +2°C and drive efforts to stay as close as possible to a +1.5°C threshold. Is such a target reachable according to the framework developed in this paper?

We base our analysis on the scenario that to us seems the most realistic we have considered so far in this paper, namely the Burke *et al.* (2015)[3] labor productivity growth together with the Dietz and Stern (2015)[6] damage function. Within this framework, the doubling in CO₂ concentration implies a temperature anomaly of 6°C (i.e., if the climate sensitivity is 6), while the increase in temperature turns out to be already about +1.52°C in 2100 even if CO₂ emissions were to remain at their 2010 level. Thus, in our set-up, there is no hope of reaching the 1.5°C target were the climate sensitivity equal to 6.

We therefore consider lower climate sensitivities ranging from 1.5 to 2.9. In this setting, we test which carbon price path could prevent the temperature anomaly from exceeding the +1.5°C ceiling. For this, we use a constant initial condition for the carbon price in 2010 (either US\$ 15, or US\$ 80) and look for the per annum growth parameter that prevents the temperature anomaly from exceeding +1.5°C in 2100.²³

²³We do not claim that the values obtained here are minimal (whatever the sense one might wish to give this here) in order to reach the +1.5°C target. At best, they are educated guesses given our numerical experience with the present model. We believe, however, that they provide a faithful indication of what a more systematic exploration of this model’s sensitivity relative to the carbon price path would provide. The latter is left for further research.

	Sensitivity of +1.5°C		Sensitivity of +2.9°C	
	Init. price of 15	Init. price of 80	Init. price of 15	Init. price of 80
Price in 2015	18.58	86.27	65.50	144.32
Price in 2020	23.00	93.04	286.02	260.35
Price in 2050	82.93	146.35	<i>xxx</i>	<i>xxx</i>

Table 8: Carbon prices preventing the temperature anomaly from reaching the 1.5°C ceiling, in (2005) US\$/tCO₂.

Table 8 provides some carbon price paths that prevent the temperature anomaly from exceeding the 1.5°C ceiling. When *xxx* is reported, the simulated values are higher than 2005 US\$ 344 (the maximum price of the backstop technology, in the same currency unit, needed to complete the energy shift), and thus meaningless. As expected, prices need to be higher in the 2.9 case than in the 1.5 case in order to reach the 1.5°C target.

The 1.5°C sensitivity case shows that the necessary carbon price increase is lower when the initial price is higher.²⁴ The price of CO₂ must reach US\$ 300 in 2080 and 2100 respectively, for an initial price of US\$ 15 and US\$ 80. This means that the energy shift should be completed around the end of the twenty-first century.

In the 2.9°C sensitivity case, despite different starting values, the value of the carbon price in 2020 must be higher than US\$ 260 per ton of CO₂. In our set-up, this implies that the energy shift should be almost completed by 2020. Needless to say, by the time this paper is written, there is little hope that the world economy will reach zero carbon emissions by 2020. Thus, we view this last result as indicating that as soon as the climate sensitivity is 2.9, it is already too late to reach the +1.5°C target.

5 Conclusion and directions for further work

By combining financial and environmental aspects, the stock-flow consistent macroeconomic model introduced in this paper allows us to evaluate economic growth, or possible (forced) degrowth, depending on the dynamics of labor productivity, damages induced by global warming, the demographic trend, and climate sensitivity, as well as the carbon price path. To our knowledge, this is the first dynamic model estimated at world level that enables both environmental and financial risks to be assessed within a framework of endogenous monetary business cycles.

Our main findings are the following: when a relatively realistic growth path for technological progress is adopted, taking due account of the influence of global warming on labor productivity, a quite (i.e., significantly convex) reasonable damage function leads to a possible breakdown of planetary magnitude either before or around the next century's turning point. Second, curbing the demographic trend does indeed postpone the potential disaster but is not sufficient to avoid it. Third, a carbon price starting at US\$ 12 t/CO₂ in 2015 and reaching US\$ 29 t/CO₂ suffices to restore perpetual growth whenever climate sensitivity is 2.9. With a high climate sensitivity of 6, a much more severe carbon price

²⁴This reflects the ongoing debate between Stern and Nordhaus, the former advocating a high starting point with a low increase in the subsequent decades, while the latter defends a low initial condition, followed by a sharper carbon price increase.

path is needed, starting for instance at US\$ 65.5 t/CO₂ in 2015 and finishing at a level higher than US\$ 285 t/CO₂ in 2050. Given the radical uncertainty that plagues climatologists' knowledge about climate sensitivity, these results call for strong and immediate action. This can take the form of a high carbon price (or price corridor, since there is no reason for the relevant incentivizing price to be uniform throughout the world), starting immediately above US\$ 65.5 t/CO₂, and rapidly increasing. Finally, it seems too late for the world economy to be able to reach the +1.5°C target, unless with a stroke of luck climate sensitivity turns out to be very low (1.5).

These results complete the path-breaking work of LtG by adding a third cause of possible collapse to the scarcity of natural resources and pollution (other than CO₂ emissions). It also *a posteriori* justifies our choice not to follow a standard cost-benefit analysis to assess the impact of climate-driven externalities. Certainly, the latter approach inevitably ends up with the issue of calibrating the “right” discount rate. While substantial efforts have been devoted to assessing whether a high or low, and sometimes a time-varying, discount rate should be considered,²⁵ none of this literature, to the best of our knowledge, has ever considered a negative rate. Yet, this possibility should be seriously envisaged. Not only because of the pervasive negative interest rates observed nowadays on international markets, but also, as shown in this paper, because a world breakdown might be the prospect that markets should start facing from now on. If the next generation is going to be less wealthy than we are today, then a US dollar today should be worth less than the same dollar in a couple of decades.

However striking our findings may be, we view them as only a preliminary step that points to a number of areas to be deepened, among which the following seem prominent:

1. In a subsequent work, we plan to couple the climate feedback loop introduced here with the modeling of non-renewable natural resource scarcity. It is only to be expected that this additional reality will cause the possible collapse to emerge sooner and more severely. It will also enable us to envision more realistic answers to be provided by the international community.
2. Here, we contented ourselves with studying business-as-usual scenarios. Our rather pessimistic conclusions by no means imply that we believe a planetary breakdown is unavoidable. First, in this paper, we have shown that certain carbon price paths can provide the appropriate incentives for a fast shift towards clean energy. This, of course, needs to be qualified considering the rather simplistic way we captured such a shift. Further work will be necessary to take due account of some of the difficulties involved in directed technological change. In particular, the problem of hysteresis due to the *ex post* non-substitutability of capital seems to us to be a key issue. The following example aptly illustrates our point: the world economy today counts approximately one billion combustion-engine vehicles, none of which can be easily converted to gas- or electric-powered vehicles. Even though a high carbon value might provide a strong incentive to develop a green mobility market, the question would still remain as to what households and industry should do with already existing cars. More generally, understanding how a world disaster may be avoided requires introducing the public sector. Public policy, however, is also constrained by public finances. The dynamic of taxes, public spending, and public debt will presumably be key in building realistic paths that can successfully circumvent the breakdown.

²⁵see, e.g., Sterner and Persson (2008)[50]

3. Even though its dynamic is already quite rich and its empirical calibration probably as accurate as possible (given current data availability constraints), the macroeconomic set-up introduced here provides but a stylized framework. We view it more as a proof of concept than a precise, prospective picture. More empirical accuracy will be gained by adding some of the following additional features:
 - Introducing some (medium-run) substitutability between capital and labor (e.g., along the lines of Grasselli *et al.*(2016)[19]) will give the model a closer fit with our daily experience, and help us understand how the productive sector might actually react more effectively to the challenges raised by global warming, as it has been assumed in the present paper;
 - Making explicit the allocation of capital, equity markets, and the banking sector (following, e.g., Giraud and Kockerols (2016)[12]) should make it possible to study in greater depth the banking sector's capacity to fund investment;
 - Dropping Say's law by decoupling supply and demand (as is the case in Grasselli and Nguyen-Huu (2016)[22]) will make it possible to understand how a more sober consumption pattern may help circumvent a disaster. On the other hand, from a Keynesian perspective, it will also enable a study of how deflation impacts the fall in demand;
 - In this paper, firms are supposed to behave myopically in the sense that aggregate investment is empirically estimated as a function of current profit. Adding expectations (e.g., adaptive ones) would allow the robustness of our findings to be checked with respect to more sophisticated behaviors;
 - Here, investment and the short-run Phillips curve are estimated using some linear OLS methods with Gaussian residuals (see Appendix E). The robustness of our findings will be checked in a companion paper, using a polynomial, non-Gaussian estimation of these aggregate behaviors.
4. In LtG, agricultural production was distinguished from industrial output, and a number of scenarios indicated that the former would decline before the latter. Understanding this timing is also crucial in order to design efficient public policies. A next step would therefore be to extend the present framework to a multisectoral macrodynamics with heterogeneous types of capital and consumption commodities.
5. As we saw above, the precise determination of the damage functions plays a crucial role in assessing the possibility of a breakdown. Even though they are borrowed from the literature, the functions employed here deserve a more careful definition. We plan to rewrite them by quantifying the economic impact of the rise in sea level, glacier melting, soil erosion, etc. This not only requires a multisectoral standpoint (see 4. above) but also a geographical disaggregation of the broad planetary perspective adopted here.

References

- [1] Population Division. World Population Prospects 2015. Data booklet, United Nations, Department of Economic and Social Affairs, Population Division, 2015.
- [2] F. Brauer and C. Castillo-Chavez. *Mathematical Models in Population Biology and Epidemiology*. Springer-Verlag, 2000.
- [3] M. Burke, S. Hsiang, and E. Miguel. Global non-linear effect of temperature on economic production. *Nature*, 527:235–39, November 2015.
- [4] C. Chiarella and C. Di Guilmi. The financial instability hypothesis: A stochastic microfoundation framework. *Journal of Economic Dynamics and Control*, 35(8):1151–71, August 2011.
- [5] M. Dell, B. F. Jones, and B. A. Olken. Temperature shocks and economic growth: Evidence from the last half century. *American Economic Journal: Macroeconomics*, 4(3):66–95, July 2012.
- [6] S. Dietz and N. Stern. Endogenous growth, convexity of damage and climate risk: How nordhaus’ framework supports deep cuts in carbon emissions. *The Economic Journal*, 125(583):574–620, 2015.
- [7] R. Feenstra, R. Inklaar, and M. Timmer. The Next Generation of the Penn World Table. *American Economic Review*, 105(10):3150–82, October 2015.
- [8] I. Fisher. The debt-deflation theory of great depressions. *Econometrica*, 1(4):337–57, 1933.
- [9] International Monetary Fund. World economic outlook: Too slow for too long. Technical report, Washington, April 2016.
- [10] O. Geoffroy, D. Saint-Martin, D. J. L. Olivié, A. Voldoire, G. Bellon, and S. Tytéca. Transient climate response in a two-layer energy-balance model. Part I: Analytical solution and parameter calibration using CMIP5 AOGCM experiments. *Journal of Climate*, 26(6):1841–57, 2013.
- [11] G. Giraud and M. R. Grasselli. Inequality, leverage and wealth in a monetary, stock-flow consistent macro-dynamics. Forthcoming 2016.
- [12] G. Giraud and T. Kockerols. Making the European Banking Union Macro-Economically Resilient: Cost of Non-Europe Report. Report to the European Parliament 2015.
- [13] G. Giraud and A. Pottier. Debt-Deflation versus the Liquidity Trap: the Dilemma of Nonconventional Monetary Policy. *Economic Theory*, 62(1):383–408, June 2016.
- [14] W. Godley and M. Lavoie. *Monetary Economics: An Integrated Approach to Credit, Money, Income, Production and Wealth*. Palgrave Macmillan UK, 2012.
- [15] R. M. Goodwin. A growth cycle. In *Socialism, Capitalism and Economic Growth*, pages 54–8. Cambridge University Press, Cambridge, 1967.

- [16] J. Gordon. The Demise of U.S. Economic Growth: Restatement, Rebuttal, and Reflections. NBER Working Papers 19895, National Bureau of Economic Research, Inc, February 2014.
- [17] M. R. Grasselli, B. Costa Lima, S. Wang, X, and J. Wu. Destabilizing a Stable Crisis: Employment Persistence and Government Intervention in Macroeconomics. *Structural Change and Economic Dynamics*, 30:30–51, 2014.
- [18] M. R. Grasselli and B. Costa Lima. An analysis of the Keen model for credit expansion, asset price bubbles and financial fragility. *Mathematics and Financial Economics*, 6(3):191–210, 2012.
- [19] M. R. Grasselli and A. Maheshwari. Testing Goodwin Growth Cycles. Forthcoming.
- [20] M. R. Grasselli and A. Nguyen-Huu. Inflation and Speculation in a Dynamic Macroeconomic Model. *Journal of Risk and Financial Management*, 8:285–310, 2015.
- [21] M. R. Grasselli and A. Nguyen-Huu. A two time scales model of monetary dynamics with variable utilization and credit investment. *Structural Changes and Economic Dynamics*, december 2015.
- [22] M. R. Grasselli and A. Nguyen Huu. Inventory dynamics in a debt-deflation model. Forthcoming 2016.
- [23] C. A. S. Hall and J. W. Day. Revisiting the Limits to Growth After Peak Oil. *American Scientist*, 18:230–7, May-June 2009.
- [24] T. Jackson and R. Webster. Limits Revisited: A review of the limits to growth debate. Technical report, APPG on Limits to Growth, 2016.
- [25] S. Keen. Finance and economic breakdown: modeling Minsky’s ”financial instability hypothesis”. *Journal of Post Keynesian Economics*, pages 607–35, 1995.
- [26] A. V. Korotayev and S. V. Tsirel. A Spectral Analysis of World GDP Dynamics: Kondratieff Waves, Kuznets Swings, Juglar and Kitchin Cycles in Global Economic Development, and the 2008–2009 Economic Crisis. *Structure and Dynamics*, 2010.
- [27] S. Kuznets. *Secular Movements in Production and Prices - Their Nature and their Bearing upon Cyclical Fluctuations*. Houghton Mifflin, Boston, MA, 1930.
- [28] T. M. Lenton, H. Held, E. Kriegler, J. W. Hall, W. Lucht, S. Rahmstorf, and H. J. Schellnhuber. Tipping elements in the earth’s climate system. *Proceedings of the National Academy of Sciences*, 23(6):1786—93, February 2008.
- [29] B. Linner and H. Selin. The united nations conference on sustainable development: forty years in the making. *Environment and Planning C: Government and Policy*, 31(6):971–87, 2013.
- [30] N.G. Mankiw. *Macroeconomics*. Worth Publishers, 2010.
- [31] A. Mas-Colell, M. D. Whinston, and J. R. Green. *Microeconomic Theory*. Number 9780195102680 in OUP Catalogue. Oxford University Press, May 1995.

- [32] J. Meadowcroft. Reaching the limits? developed country engagement with sustainable development in a challenging conjuncture. *Environment and Planning C*, 31(6):988–1002, 2013.
- [33] D. H. Meadows and Club of Rome. *The Limits to growth: a report for the Club of Rome’s project on the predicament of mankind*. Number vol. 1974,ptie. 2 in *The Limits to Growth: A Report for the Club of Rome’s Project on the Predicament of Mankind*. New American Library, 1974.
- [34] D.H. Meadows, Club of Rome, and Potomac Associates. *The Limits to growth: a report for the Club of Rome’s project on the predicament of mankind*. Number ptie. 1 in Potomac Associates book. Universe Books, 1972.
- [35] S. Motesharrei, J. Rivas, and E. Kalnay. Human and nature dynamics (handy): Modeling inequality and use of resources in the collapse or sustainability of societies. *Ecological Economics*, 101:90 – 102, 2014.
- [36] A. Nguyen-Huu and B. Costa-Lima. Orbits in a stochastic Goodwin–Lotka–Volterra model. *Journal of Mathematical Analysis and Applications*, 419(1):48–67, November 2014.
- [37] W. D. Nordhaus. Optimal Greenhouse-Gas Reductions and Tax Policy in the ‘Dice’ Model. *American Economic Review*, 83(2):313–17, May 1993.
- [38] W. D. Nordhaus. A Review of the ”stern review on the economics of climate change”. *Journal of Economic Literature*, 45(3):686–702, 2007.
- [39] W. D. Nordhaus. Estimates of the social cost of carbon: Concepts and results from the dice-2013r model and alternative approaches. *Journal of the Association of Environmental and Resource Economists*, 1(1), 2014.
- [40] W. D. Nordhaus and P. Sztorc. *DICE 2013R: Introduction and User’s Manual*, October 2013.
- [41] R. S. Pindyck. The Use and Misuse of Models for Climate Policy. NBER Working Papers 21097, National Bureau of Economic Research, Inc, April 2015.
- [42] S. Ryoo. Long waves and short cycles in a model of endogenous financial fragility. *Journal of Economic Behavior & Organization*, 74(3):163–86, 2010.
- [43] C. H. Dos Santos. A stock-flow consistent general framework for formal minskyan analyses of closed economies. *Journal of Post Keynesian Economics*, 27(4):712–35, 2005.
- [44] V. J. Schwanitz. Evaluating integrated assessment models of global climate change. *Environmental Modelling & Software*, 50:120–31, December 2013.
- [45] S. C. Sherwood and M. Huber. An adaptability limit to climate change due to heat stress. *Proceedings of the National Academy of Sciences*, 107(21):9552–55, 2010.
- [46] F. Smets and R. Wouters. Shocks and Frictions in US Business Cycles: A Bayesian DSGE Approach. *American Economic Review*, 97(3):586–606, June 2007.

- [47] E. A. Stanton, F. Ackerman, and S. Kartha. Inside the integrated assessment models: Four issues in climate economics. *Climate and Development*, 1(2):166–84, July 2009.
- [48] N. Stern. *Stern Review: The economics of climate change*, volume 30. HM treasury London, 2006.
- [49] N. Stern. The structure of economic modeling of the potential impacts of climate change: Grafting gross underestimation of risk onto already narrow science models. *Journal of Economic Literature*, 51(3):838–59, September 2013.
- [50] T. M. Sterner and U. M. Persson. An even sterner review: Introducing relative prices into the discounting debate. *Review of Environmental Economics and Policy*, 2(1):61–76, 2008.
- [51] T. F. Stocker, D. Qin, G. Plattner, M. Tignor, S. K. Allen, J. Boschung, A. Nauels, Y. Xia, V. Bex, and P. M. Midgley. Climate change 2013: The physical science basis. Technical report, 2013. 1535 pp.
- [52] R. S. J. Tol. The economic effects of climate change. *Journal of Economic Perspectives*, 23(2):29–51, June 2009.
- [53] G. M. Turner. A comparison of The Limits to Growth with 30 years of reality. *Global Environmental Change*, 18:397–411, 2008.
- [54] G. M. Turner. Are we on the cusp of collapse? Updated comparison of The Limits to Growth with historical data. *Gaia: Ökologische Perspektiven in Natur-, Geistes- und Wirtschaftswissenschaften*, 21(2):116–24, June 2012.
- [55] G. M. Turner. Is Global Collapse Imminent? Mssi research paper no. 4, Melbourne Sustainable Society Institute, The University of Melbourne, 2014.
- [56] P. J. Verdoorn. *Productivity Growth and Economic Performance: Essays on Verdoorn’s Law*, chapter Factors that Determine the Growth of Labour Productivity, pages 28–36. Palgrave Macmillan UK, London, 2002.
- [57] M. L. Weitzman. Fat-tailed uncertainty in the economics of catastrophic climate change. *Review of Environmental Economics and Policy*, 5(2):275–292, 2011.
- [58] M. L. Weitzman. Ghg targets as insurance against catastrophic climate damages. *Journal of Public Economic Theory*, 14(2):221–44, 2012.

Appendices

The Appendices are ordered as follows: i) the description of the empirical data we constructed for the model estimation; ii) the calibration of the temperature dynamic; iii) the estimation of the demographic scenario; and iv) the calibration of the climate module.

A Data collection

To estimate the parameters of the model at the global level, we collected historical data representing more than 80% of the world's GDP. Since global aggregate data are not available through open source, we collected the data at country level.

The final sample is based on the data of 36 countries. It includes 18 members of G20,²⁶ 16 members of OECD that are not individually part of the G20,²⁷ and two non-OECD countries.²⁸ The combined GDP of the listed countries accounted for 87% of world GDP in 2014.²⁹ At the time we were collecting our data, there was a lack of data on capital stock and wages after 2011, so we limited our time frame to the period 1991-2011. A detailed description of the methodology used to construct the database is given below.

1. **The World Bank World Development Indicators database** provides most of the data required to estimate the parameters for the model. All the data for absolute values are in current local currency units and converted to PPP using the conversion ratio for comparability.

- **Nominal GDP** is formed as a sum of the two variables: *Gross value added at factor cost* and *Net taxes on products*, since the aggregate time series for the considered list of countries is not available. The only country for which GDP was considered directly is China, as GDP-at-factor-cost data are unavailable. GDP-at-factor-cost data are largely available for the entire considered period, except in the case of Argentina and Indonesia. It is important to mention that the missing data point for the Argentinian economy is the PPP conversion factor, not the GDP at factor cost or net taxes. Taking into account the volatility of the Argentinian peso, it is impossible to make any assumptions on the behavior of the conversion rate. The missing data points for the GDP at factor cost and net taxes, both here and later in this subsection, are thus filled in by assuming that the Argentinian share (e.g., GDP at factor cost) of the total 36 countries considered (in this case, the GDP at factor cost of 36 countries) remains stable. The data for Indonesia are available only from 2010. The missing data for 1991-2009 are thus projected through linear regression of the data available for the 2010-2014 time frame. Likewise, net tax data are missing for Indonesia and filled in using the same method described above for GDP at factor cost. Additionally, net tax data are missing for the USA

²⁶Argentina, Australia, Brazil, Canada, China, France, Germany, India, Indonesia, Italy, Japan, South Korea, Mexico, Russia, South Africa, Turkey, the United Kingdom, and the United States.

²⁷Austria, Belgium, Czech Republic, Denmark, Finland, Greece, Hungary, Ireland, Luxembourg, Netherlands, Norway, Poland, Portugal, Spain, Sweden, and Switzerland.

²⁸Singapore and Hong Kong, the latter being considered as a country for the purpose of this study.

²⁹Global GDP is taken from the World Development Indicators database, as released in 2016.

in 1991-1996 and Hong Kong in 1991-1999. The missing data were also built using linear regression.

- **GFCF** or *Gross fixed capital formation* is the variable that captures the level of investment in the economy and is defined by the World Bank as follows: "Gross fixed capital formation (formerly gross domestic fixed investment) includes land improvements (fences, ditches, drains, and so on); plant, machinery, and equipment purchases; and the construction of roads, railways, and the like, including schools, offices, hospitals, private residential dwellings, and commercial and industrial buildings. According to the 1993 SNA, net acquisitions of valuables are also considered capital formation". This variable is available for all the countries listed, except Argentina, for which the only available data point is for 2011 due to the lack of a conversion factor, as mentioned above. As for the earlier missing values, these were estimated using the overall ratio of Argentinian GFCF to the total GFCF for the 36 countries.
- **Household final consumption expenditure** (formerly private consumption) as defined by the World Bank is: "the market value of all goods and services, including durable products (such as cars, washing machines, and home computers), purchased by households. It excludes purchases of dwellings but includes imputed rent for owner-occupied dwellings. It also includes payments and fees to governments to obtain permits and licenses. Here, household consumption expenditure includes the expenditures of nonprofit institutions serving households, even when reported separately by the country." Household consumption in PPP dollars is not available directly for Argentina, so this was calculated via the available ratio of the Argentinian household consumption to the total household consumption of the 36 countries.
- **The employment rate** for the 36 countries considered was calculated as the percentage of employed population within the 15-64 age group. This was a two-step method: firstly, the number of people within the 15-64 age group was calculated from the percentage of the total population data and, secondly, the number of employed persons was calculated using data on the share of the employed population within the 15-64 age group.
- **GDP deflator (index)** is calculated as the ratio of the country's GDP in current prices to its GDP in constant prices. Both data sets are available through the World Bank World Development Indicators database for all 36 countries considered.

2. **The Penn World Table** provided data on capital stock and the share of employees' wages in the economy.

- **Capital stock** data are already provided in PPP dollar units and available directly for all 36 countries.
- **Employee compensation** is calculated from the share of labor compensation in GDP available through the World Penn Tables. The share of labor compensation in GDP is available for all 36 countries except Russia. The average of the respective shares for Kazakhstan, Ukraine, and Belarus is taken as a proxy to calculate employee compensation in Russia.

3. **The BIS Statistics Explorer** provides data on government, private and household debt. The missing data are filled in using the World Bank World Development Indicators database and the Economic Commission for Latin America and the Caribbean database, CEPALSTAT.

- *Corporate debt* represents total credit to the non-financial corporate sector and is also defined as a percentage of GDP. The linear regression method was applied in order to fill in the missing data for: Brazil, Czech Republic, Luxembourg, Poland and Russia.

B Temperature dynamics

The temperature dynamics is based on the continuous-time, two-layer model described in Geoffroy *et al.* (2013)[10],

$$\begin{cases} \overline{C}\dot{T} = F - (RF)T - \gamma^*(T - T_0), \\ C_0\dot{T}_0 = \gamma^*(T - T_0). \end{cases}$$

Nordhaus (1993)[37] published what was to be his seminal model of greenhouse-gas emissions: the DICE model. In DICE, the two-layer model is used in a discrete formulation. In the present study, the parameters for the continuous-time model are calibrated based on the CO₂ trajectories reported in the technical report by Nordhaus *et al.* (2013)[40] p.30, and thus the global temperature change trajectories, p.31.

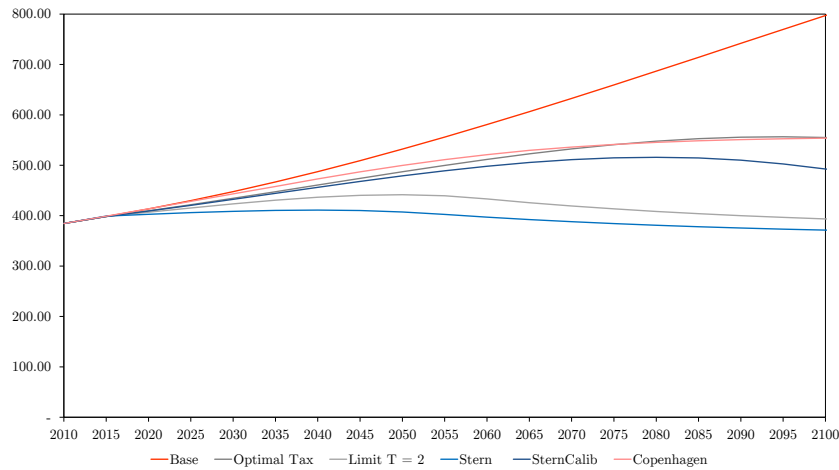


Figure 22: CO₂ concentration in ppm under different scenarios. Source: Nordhaus (2013)[40], p.30.

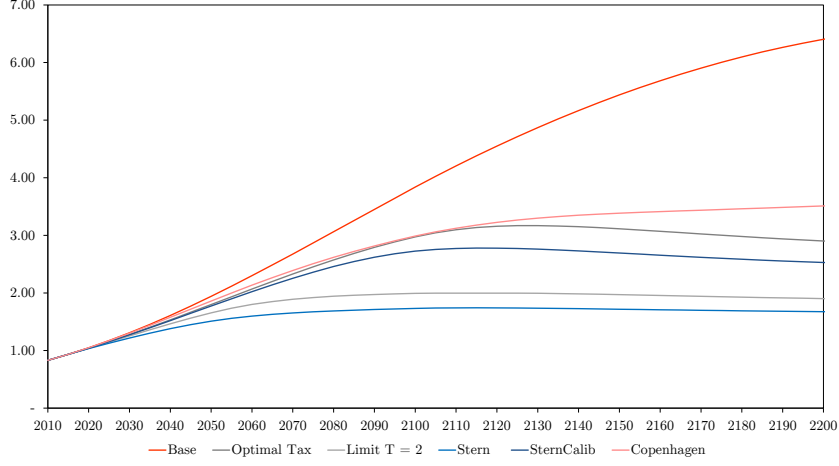


Figure 23: Temperature change under different scenarios. Source: Nordhaus (2013)[40], p.31.

To identify the two-layer model in its discrete version as described by Nordhaus (2013)[40], the system is

$$\begin{cases} \dot{T} = \zeta_1 (F - \zeta_2 T - \zeta_3 (T - T_0)) \\ \dot{T}_0 = \zeta_4 (T - T_0). \end{cases}$$

One can identify the two models so that $\zeta_1 = \frac{F}{C}$, $\zeta_2 = \frac{RF}{C}$, $\zeta_3 = \frac{\gamma^*}{C}$, and $\zeta_4 = \frac{\gamma^*}{C_0}$. The equilibrium value $\zeta := 3.8/2.9$ is not calibrated according to the DICE trajectory as it represents an equilibrium value of the impact of a doubled CO_2 concentration in the atmosphere. While the endogenous radiative forcing is similar to Geoffroy (2013)[10], an additional feature is incorporated with an exogenous forcing so that

$$F(t) = \frac{F_{2 \times \text{CO}_2}}{\log(2)} \log \left(\frac{C_{\text{CO}_2(t)}}{C_{\text{CO}_2(t_0)}} \right) + F_{exo}(t).$$

Firstly, as usual, the parameter $F_{2 \times \text{CO}_2} = 3.8$. Secondly, CO_2 is the major but not the sole cause of global warming. Future warming is also projected to come from other long-lived greenhouse gases, aerosols, and other factors. As in DICE, we assume that they are controlled exogenously following the process

$$\dot{F}_{exo} = \delta_{F_{exo}} F_{exo} \left(1 - \frac{F_{exo}}{0.7} \right).$$

In 2100, 0.7 W/m^2 is the estimated non- CO_2 forcing, and the value in 2010 is 0.25 W/m^2 . In DICE 2013 code, this function is supposed to grow linearly until 2100 and then become constant at 0.7. To approximate this behavior smoothly, the parameter $\delta_{F_{exo}}$ will be 0.25, and the yearly starting values will be as indicated in Table 9,

Year	2010	2011	2012	2013	2014	2015	2016	2017	2018	2019
Value	0.25	0.26	0.27	0.28	0.29	0.30	0.31	0.32	0.33	0.34

Table 9: Starting values for the exogenous forcing dynamics.

The Nordhaus DICE model is calibrated for a five-year time mesh, whereas our calibration is designed for one year. To ensure consistency with our time mesh, we infer the

parameters $(\zeta_1, \zeta_3, \zeta_4)$ to ensure a minimal distance between their trajectories and those displayed in Figure 23.³⁰

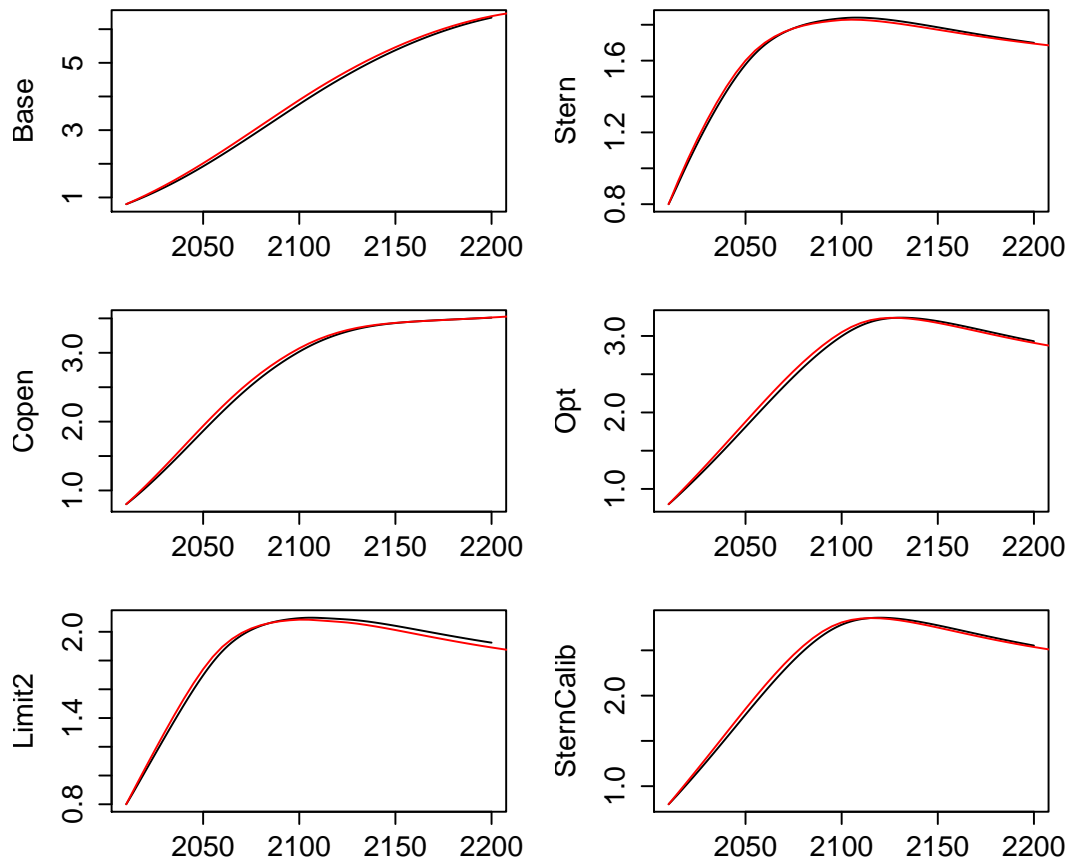


Figure 24: Fitting of the parameters for the continuous system to the discrete counterpart. In black, the simulated values with the continuous-time system. In red, the DICE temperature increase.

Parameter	Value
ζ_1	0.019716867
ζ_3	0.125815568
ζ_4	0.007654311

Table 10: Estimated values of the zetas for the continuous-time system.

C The demographic scenario

The working-age population is assumed to grow according to some logistic function,

$$\frac{\dot{N}}{N} = q \left(1 - \frac{N}{M} \right).$$

³⁰The methodology involves finding the set of parameters that produces trajectories as close as possible to the values generated by DICE. For the sake of clarity, the values found will minimize the Euclidean distance via implementation of a BFGS algorithm.

In order to infer the parameters (q , the speed rate, and, M , the upper limit), we minimize the distance between the simulated process and the United Nations median fertility scenario using a BFGS algorithm.³¹

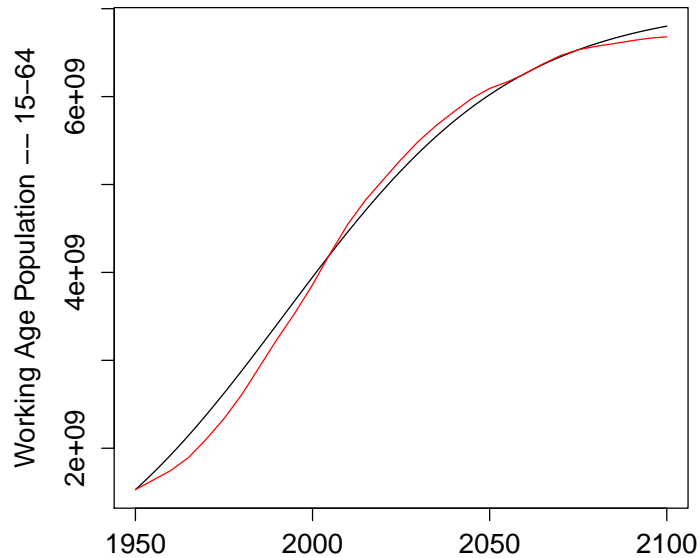


Figure 25: Fitting of the simulated scenario to the 15-64 age group scenario. Source: United Nations.

Figure 25 shows the fitting of the logistic function (in black) to the United Nations time series (in red). The parameters are displayed in Table 11.

Parameter	Value
q	0.0305
M	7,055,925,493

Table 11: Calibrated parameters.

D CO₂ dynamics

The measures of the carbon cycle are in gigatons of carbon (hereafter GtC) for CO₂ concentration, and emissions are measured in gigatons of CO₂ (hereafter GtCO₂). For the sake of clarity, Table 12 shows the conversion factor of the different carbon cycle units. It displays three units: GtC, GtCO₂, and part per million (hereafter ppm).

³¹The time series for the working-age population is the median fertility scenario for the 15-64 age group.

From \ To	GtC	GtCO ₂	ppm
1 GtC	1	3.664	1/2.13
1 GtCO ₂	1/3.664	1	1/7.81
1 ppm	2.13	7.81	1

Table 12: Conversion table for carbon cycle metrics.

According to Nordhaus (2013)[40], the =CO₂ accumulates in three layers: (i) the atmosphere; (ii) a mixing reservoir in the upper oceans and the biosphere; and (iii) the deep ocean. This mechanism is represented by the system

$$\begin{pmatrix} \dot{\text{CO}}_2^{AT} \\ \dot{\text{CO}}_2^{UP} \\ \dot{\text{CO}}_2^{LO} \end{pmatrix} = \begin{pmatrix} E \\ 0 \\ 0 \end{pmatrix} + \underbrace{\begin{pmatrix} \phi_{11} & \phi_{12} & \phi_{13} \\ \phi_{21} & \phi_{22} & \phi_{23} \\ \phi_{31} & \phi_{32} & \phi_{33} \end{pmatrix}}_{:=\Phi} \begin{pmatrix} \text{CO}_2^{AT} \\ \text{CO}_2^{UP} \\ \text{CO}_2^{LO} \end{pmatrix},$$

The coefficients of matrix Φ are linked together as follows:

$$\Phi = \begin{pmatrix} -b_{12} & b_{12} \frac{C_{ATeq}}{C_{UPeq}} & 0 \\ b_{12} & -b_{12} \frac{C_{ATeq}}{C_{UPeq}} - b_{23} & b_{23} \frac{C_{UPeq}}{C_{LOeq}} \\ 0 & b_{23} & -b_{23} \frac{C_{UPeq}}{C_{LOeq}} \end{pmatrix},$$

where b_{ij} is the flow of CO₂ between the layers i and j , and C_{ieq} is the equilibrium concentration of the layer i , constant for the modeling.

A discrete version of this system described by Nordhaus (2013)[40] is more intuitive in terms of CO₂ flows into the atmospheric layer and flows between the layers,

$$\begin{pmatrix} \text{CO}_2^{AT}(t) \\ \text{CO}_2^{UP}(t) \\ \text{CO}_2^{LO}(t) \end{pmatrix} = \begin{pmatrix} E(t) \\ 0 \\ 0 \end{pmatrix} + \begin{pmatrix} 1 - b_{12} & b_{12} \frac{C_{ATeq}}{C_{UPeq}} & 0 \\ b_{12} & 1 - b_{12} \frac{C_{ATeq}}{C_{UPeq}} - b_{23} & b_{23} \frac{C_{UPeq}}{C_{LOeq}} \\ 0 & b_{23} & 1 - b_{23} \frac{C_{UPeq}}{C_{LOeq}} \end{pmatrix} \begin{pmatrix} \text{CO}_2^{AT}(t-1) \\ \text{CO}_2^{UP}(t-1) \\ \text{CO}_2^{LO}(t-1) \end{pmatrix}.$$

The DICE model is calibrated for a five-year time mesh, whereas our calibration is designed for one year. To have parameters consistent with our time mesh, we calibrate b_{12} and b_{23} so that the continuous trajectories obtained with these parameters minimize the distance from the discrete counterpart of Nordhaus' DICE model, as displayed in Figure 26.

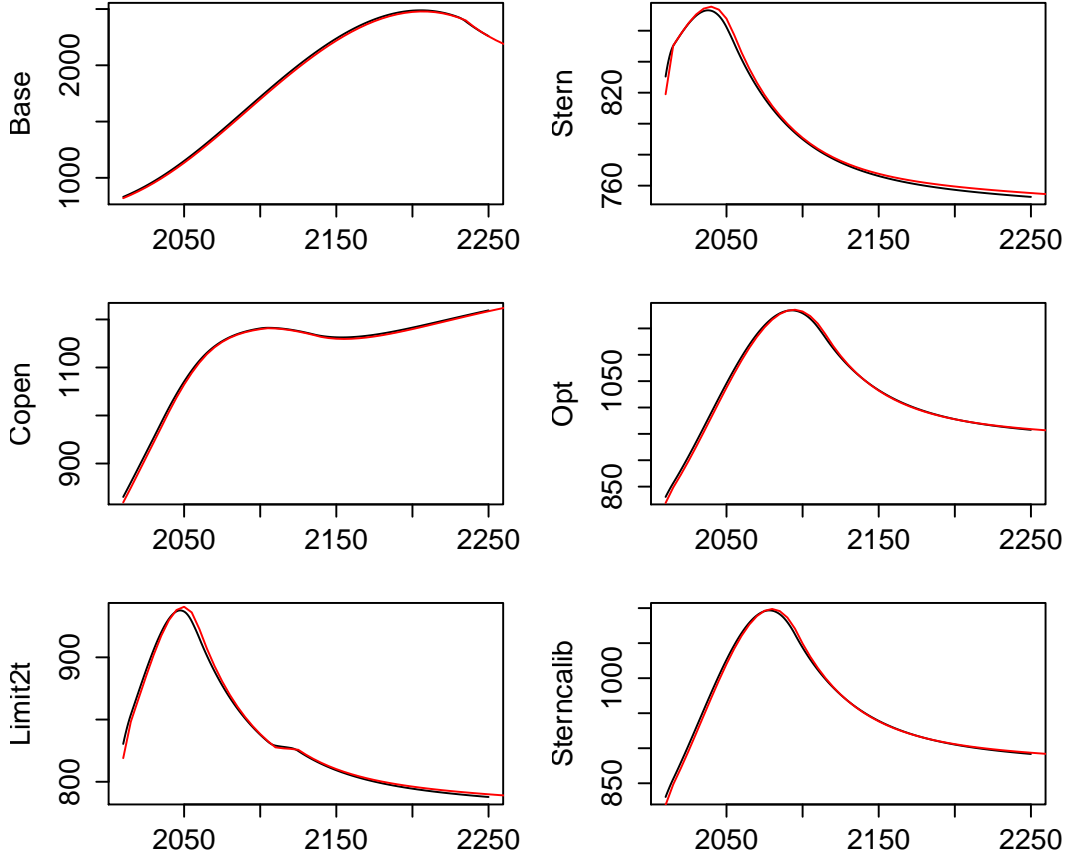


Figure 26: Fitting of the parameters for the continuous system to the discrete counterpart. In black, the simulated values with the continuous-time system. In red, the DICE CO₂ accumulation in the atmosphere.

In other words, our estimates minimize the Euclidean distance between our continuous simulation and the trajectories interpolated from the DICE model, which served as a reference, meaning,

$$(\hat{b}_{12}, \hat{b}_{23}) = \operatorname{argmin}_{(b_{12}, b_{23})} d(\text{obs}, \text{sim}(b_{12}, b_{23}, C_{AT_{eq}}, C_{UP_{eq}}, C_{LO_{eq}})),$$

where *obs* is the vector of observation of the DICE model over the 2010-2250 period, $\text{sim}(b_{12}, b_{23}, C_{AT_{eq}}, C_{UP_{eq}}, C_{LO_{eq}})$ is the corresponding vector taken from the simulation using the couple (b_{12}, b_{23}) as the argument of the estimation and the constants $(C_{AT_{eq}}, C_{UP_{eq}}, C_{LO_{eq}})$, and *d* is the Euclidean distance. Using a BFGS algorithm, we obtain the estimated values given in Table 13.

Parameter	Value
b_{12}	0.01727393
b_{23}	0.00050000

Table 13: Calibrated parameters.

E Estimation of the macroeconomic dynamics

The estimations that follow are based on the data defined in Appendix A.

E.1 The capital-to-output ratio – ν

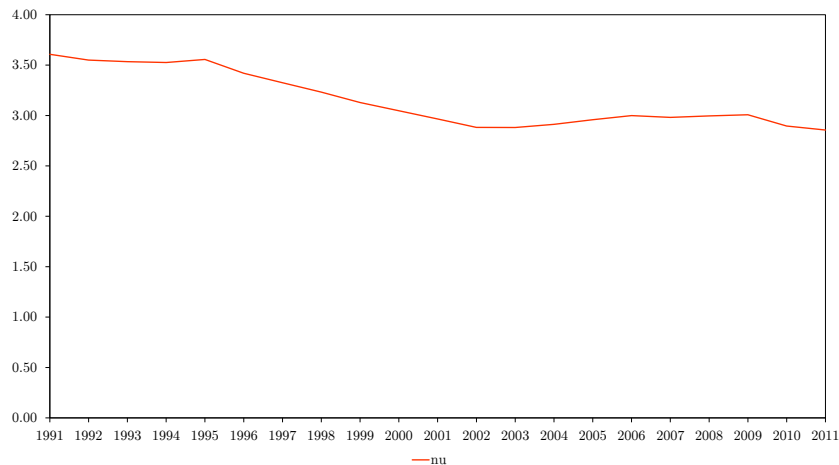


Figure 27: Capital-to-output ratio from 1990 to 2011.

Figure 27 shows the capital-to-output ratio, ν , over time. Note that ν is not constant, although roughly stable after 2000 at an average of 2.9485. This value is in line with previous findings or assumptions (see Appendix C in Feenstra *et al.* (2015)[7] or the AMECO database, which assume an initial value of capital-to-output ratio of 3 in 1960).

E.2 Labor productivity – a_t

For the different labor productivity scenarios, the estimation below helped us develop our baseline scenario. Figure 28 shows the growth rate over time of labor productivity. For its inference, we do not use the OLS regression as suggested in Grasselli *et al.* (2016)[19],

$$\log(a_t) = \log(a_0) + \beta t + \varepsilon_t,$$

because the low growth rates in the early 1990s would strongly bias the estimate of the slope β . For a better approximation, we thus infer α so that it equals the mean value of the time series, i.e., 0.0226.

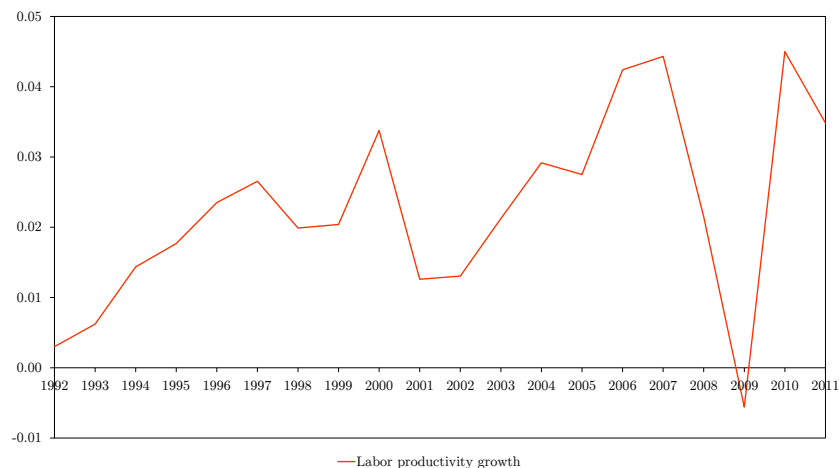


Figure 28: The labor productivity growth rate from 1990 to 2011.

E.3 The short-term Phillips curve

In order to calibrate an aggregate short-term Phillips curve, we estimate the model

$$\frac{\dot{w}}{w} = \phi_0 + \phi_1 \lambda,$$

where w denotes the nominal wage rate, λ the employment rate, ϕ_0 the intercept, and ϕ_1 the slope of the aggregate function.

For each country, the data are taken from the sources presented in Appendix A. The employment rate, λ , is taken as given, while the wage per capita, w , is computed as the total wage bill divided by the labor force.

Due to the very low volatility of the data at an aggregate level (the aggregate employment rate, λ , ranges from 0.69 to 0.73),³² no significant econometric estimate could be made at this level of aggregation. As a result, a panel data regression analysis was used for the 36 selected countries to improve the inference. In order to cope with temporal autocorrelation and omitted variables, the "first-difference" model was selected to estimate the slope of the function. The estimated model is as follows:

$$\left(\frac{\dot{w}}{w}\right)_{it} \sim \lambda_{it},$$

where i denotes the country and t the year of estimation. Note that we constrain the intercept to be zero.

Using the *plm* package (free *R* software), we obtain significant results, presented in Table 14.

Coefficient	Estimate	Std Error	t-value	Pr(> t)	Observations
ϕ_1	1.08519	0.29034	3.7376	0.0002013***	720

Table 14: First-difference panel regression of the short-term Phillips curve over the period 1991-2010. Sources: World Bank, Penn.

Next, given the estimated slope for the aggregate wage function, we calibrate the intercept in order to match the empirical first moment of the sample,

$$\mathbb{E}\left(\frac{\dot{w}}{w}\right) = \phi_0 + \phi_1 \mathbb{E}(\lambda).$$

Finally, we obtain the following relation for the short-term Phillips curve:

$$\frac{\dot{w}}{w} = -0.735026 + 1.08519\lambda.$$

Figure 29 presents the real and fitted wage curves and highlights the robust behavior of the estimation. The Kolmogorov-Smirnov test does not accept the null hypothesis of Gaussian residuals. However, the qualitative results are displayed in Figure 29, the estimation of a model with a non-Gaussian distribution being left for further research.

³²Strongly driven by India and China in terms of population size.

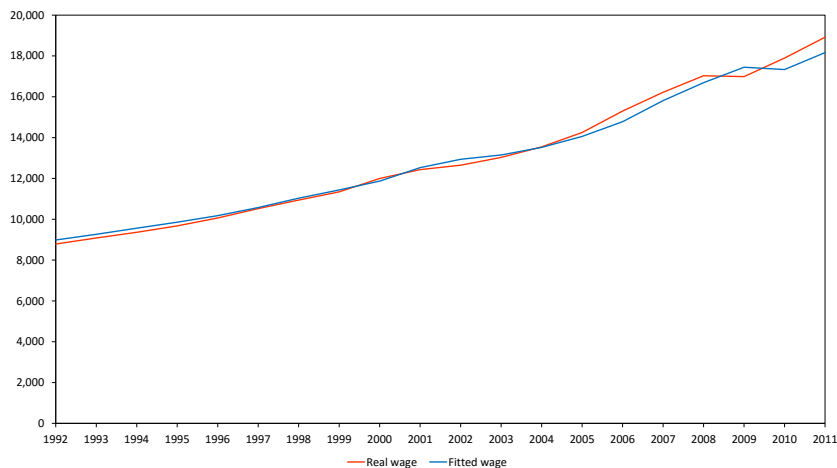


Figure 29: Observed and fitted wage curve over the period 1992-2010. Sources: World Bank, Penn.

Note that we conducted the same panel regression analysis taking both the employment rate λ and the inflation i of each country in the sample as explanatory variables. Inflation was computed as the growth of the GDP deflator presented in Appendix A. The p -value of 0.77 for the inflation parameter shows that the null hypothesis of this parameter being zero is not rejected. After this model selection process, we thus only consider the specification of the short-term Phillips curve with λ as the sole explanatory variable for our calibration, and we assume complete monetary illusion.³³

Coefficient	Estimate	Std Error	t-value	Pr(> t)	Observations
ϕ_λ	1.07991	0.29111	3.7096	0.0002245***	720
ϕ_i	0.00062	0.00217	0.2891	0.7725579	720

Table 15: First-difference panel regression of the short-term Phillips curve with λ and i as explanatory variables over the period 1991-2010. Sources: World Bank, Penn.

As a caveat, we should point out that residuals that are autocorrelated.

E.4 The investment function

In order to calibrate the aggregate investment function, we estimate the following model:

$$\frac{I}{Y} = i_0 + i_1\pi,$$

where I is real investment, Y is real output, π is the profit share, i_0 is the intercept, and i_1 is the slope of the aggregate function.

The data are drawn from the sources previously mentioned in Appendix A. Output Y and investment I are taken as given (we use GDP at factor cost as government is not modeled). We must point out that, due to data availability issues, we use these nominal frameworks and assume constant price relativity for the identification. The profit

³³It is worth mentioning that the constant parameter incorporates the information that wages reset automatically, given a constant inflation rate.

share, π , is computed as the ratio of GDP at factor cost net of wages (gross profit) and net of interest payments on debt. As we have information only about the level of debt for the 36 countries selected, we assume a constant interest rate of 3% for our calculations.

Using the free *R* software, we estimate the following model on aggregate series of the 36 selected countries with an ordinary least square (OLS) regression:

$$\left(\frac{I}{Y}\right)_t \sim \pi_t.$$

Table 16 presents the significant results of the estimation. A Kolmogorov-Smirnov test applied to the normality of the residuals shows a p -value of 0.4448. Hence, with a 95% confidence band, this test does not reject the null hypothesis of the normality of the errors.

Coefficient	Estimate	Std. Error	t-value	Pr(> t)	Observations
i_0	0.04260	0.01288	3.308	0.0037**	36
i_1	0.64153	0.03773	17.002	5.96e-13***	36

Table 16: OLS regression of the investment function over the period 1991-2011. Sources: World Bank, Penn.

Finally, we obtain the following relation:

$$\frac{I}{Y} = 0.04260 + 0.64153\pi.$$

Figure 30 presents the real and fitted wage curves and highlights the robust behavior of the estimation. Note that no issues regarding the residuals were identified for this estimation. Indeed, a Kolmogorov-Smirnov test applied to the normality of the residuals shows a p -value of 0.4448. Hence, this test does not reject the null hypothesis of the normality of the errors.

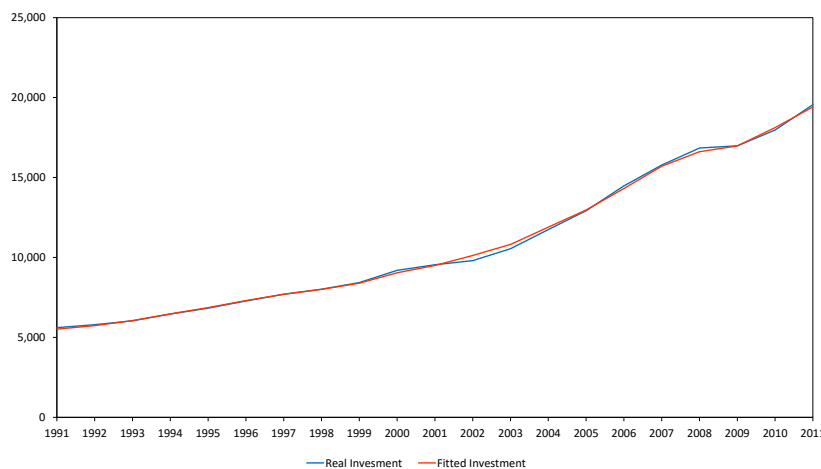


Figure 30: Observed and fitted investment curve over the period. 1992-2010 Sources: World Bank, Penn.

E.5 The debt accumulation function

As shown by Figure 31, a mismatch exists between observed debt accumulation and observed investment net of profits. Indeed, firms may become indebted for purposes other than investing, as for instance, for speculative reasons (note the singular pattern during the financial bubble over the period 2000-2007), for distributing dividends or paying taxes. By way of illustration, the US monetary-dividend-to-GDP ratio presented below appears to be highly correlated with the debt-variation-to-GDP ratio and its level in line with the corresponding estimated parameter presented below.

In order to reconcile the model with the data, a corrective term was added to the debt accumulation function, becoming

$$\dot{D} = \text{div } pY + pI - \Pi,$$

where d_{fi} denotes “the gray debt” or, in other words, can be considered as the dividends and/or taxes paid by the firms to the state.

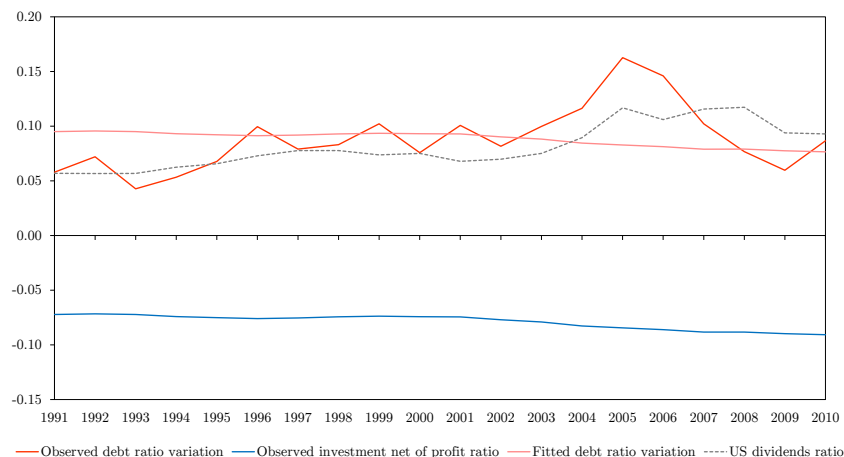


Figure 31: Observed aggregate debt variation (red curve) and investments net of profit (blue curve), fitted aggregate debt variation (light red curve) and US monetary dividend (gray dotted curve) over the period 1991-2010 (all as ratios of GDP). Sources: World Bank, Penn, BEA.

The constant, div , was calibrated to reconcile the first moments of the debt accumulation function with respect to the data, that is,

$$\mathbb{E} \left(\frac{\dot{D}}{pY} \right) = \text{div} + \mathbb{E} \left(\frac{pI}{pY} - \pi \right).$$

We used the fitted value of investment for the calculation in order to obtain the best fit for our model, and found a value of 0.1672287 for div .

E.6 The depreciation rate of capital – δ

Due to the lack of identification, the depreciation rate of capital is often calibrated as an educated guess (see Smets and Wouters (2007)[46] among others). In the presented

model, one of the drivers of the real output growth rate is the law of motion of capital,

$$\frac{\dot{K}}{K} = \frac{\kappa(\pi)}{\nu} - \delta.$$

Having previously calibrated $\kappa(\pi)$ and ν , we now calibrate δ so that the right-hand side of the equation matches the real growth rate of GDP:

$$\mathbb{E} \left[\frac{\kappa(\pi)}{\nu} - \frac{\dot{Y}}{Y} \right] = \hat{\delta}.$$

By doing so, we find $\hat{\delta} = 0.0645$.

E.7 The price dynamics

The price dynamics model is represented as follows:

$$\frac{\dot{p}}{p} = \eta_p(m\omega - 1) + c,$$

where $\eta_p, c > 0$ and $m \geq 1$. In this relationship, we identify c to some long-term inflation rate and $\eta_p(m\omega - 1)$ to some frictional inflation. In other words, and for the purpose of the estimation, we assume that

$$\mathbb{E}(\eta_p(m\omega - 1)) = 0,$$

so that

$$c = \mathbb{E} \left(\frac{\dot{p}}{p} \right).$$

Using the first relation, we calibrate m as

$$m = \frac{1}{\mathbb{E}(\omega)},$$

and immediately obtain c from the second relation.

η_p being set, we focus on the temporary component of inflation and calibrate η_p such that short-term inflation does not exceed 0.05 in absolute terms,³⁴ for the sake of precision, the calibration is made by assuming the wage share ω to be contained in a reasonable range, that is $[0.24, 1]$.

Table 17 summarizes the calibration retained for the numerical simulations. The data are taken from the previously presented sources and the estimation was carried out for the period 1991-2011.

Parameter	Value
c	0.030322
m	1.609972
η_p	0.0819709341

Table 17: Calibration of the price dynamics parameters Source: World Bank

³⁴For the sake of clarity, inflation is contained within the set $[-0.05 + c; 0.05 + c]$.